

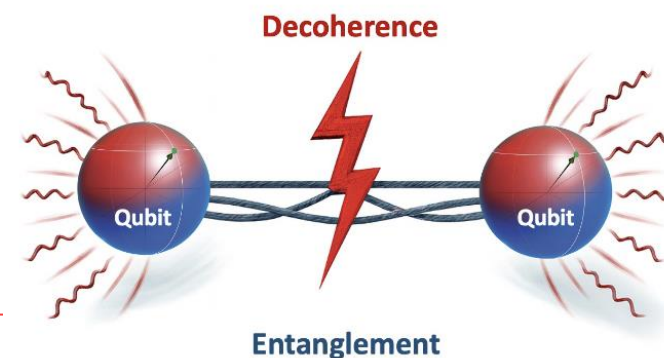


Quantum entanglement and decoherence using top quark pairs

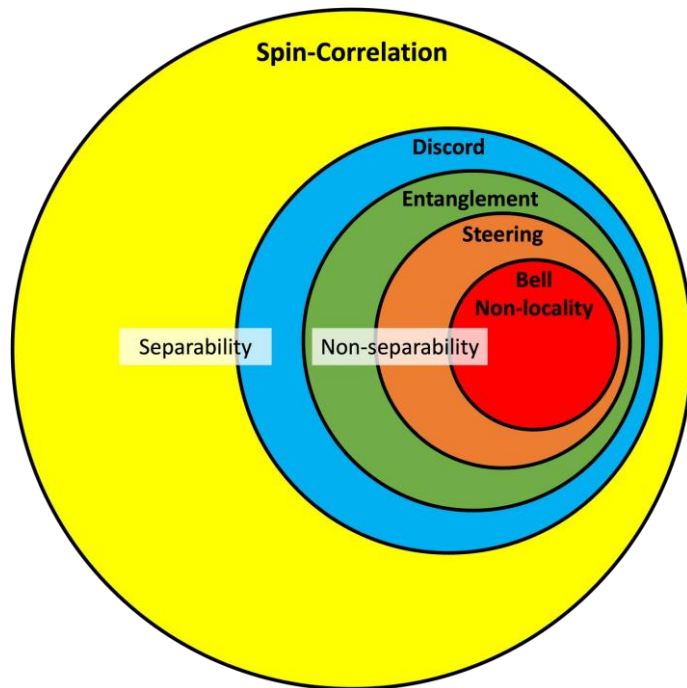
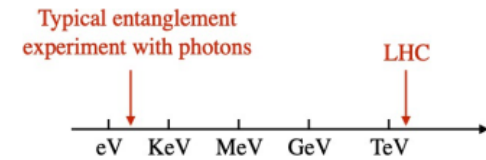
José Manuel Camacho, María Moreno Llácer & Marcel Vos (IFIC, CSIC-UV)

Work in progress with Rafael Aoude (U. Edinburgh), Fabio Maltoni (U. Bologna+Louvain), Leonardo Satrioni (U. Louvain)

Valencia, Nov. 2025



- LHC data offer a new way to test experimentally the fundamental principles of quantum mechanics at very high energies
- One of such tests involves **quantum entanglement**
 - Observation reported by both ATLAS and CMS experiments in events with top quark pairs
 - Ongoing studies in the Higgs sector as well
- There are other concepts from quantum computation that can be explored at the LHC
 - One is “**magic**” (or “non-stabiliserness” of quantum states, 2^{nd} stabilizer Renyi entropy)

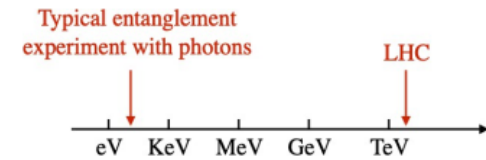


- Spin correlation: → *found in Run-1*
Statistical classical correlation between spins
- Quantum discord:
Quantum correlations yet in separables states
- Quantum entanglement: → *what we will talk about today*
Subsystems are not separable
- Steering:
Measurement in one subsystem influences the other
- Bell non-locality: → *will we ever get there?*
 - Correlation cannot be described by local hidden variables
 - Are the effects strong enough to violate Bell's inequalities?

more
stringent
tests



- LHC data offer a new way to test experimentally the fundamental principles of quantum mechanics at very high energies
- One of such tests involves **quantum entanglement**
 - Observation reported by both ATLAS and CMS experiments in events with top quark pairs
 - Ongoing studies in the Higgs sector as well
- There are other concepts from quantum computation that can be explored at the LHC
 - One is “**magic**” (or “non-stabiliserness” of quantum states, 2^{nd} stabilizer Renyi entropy)



Recent LHC results:

- **Observation of quantum entanglement at production threshold**

[1] [Nature 633 \(2024\) 542](#) [by ATLAS]

[2] [Rep. Prog. Phys 87 \(2024\) 117801](#) [by CMS]

- **Observation of quantum entanglement in the boosted regime**

[3] [Phys. Rev. D 110 \(2024\) 112016](#) [by CMS]

- **Measurements of polarization and spin correlation**

[3] [Phys. Rev. D 110 \(2024\) 112016](#) [by CMS]

- **Observation of magic states of top quark pairs**

[4] [CMS PAS TOP-25-001](#) [by CMS]



The top quark is special

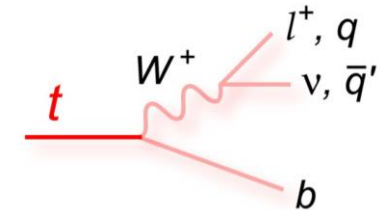
Most massive elementary particle known to date - very short lifetime -

$$\tau_t = 1/\Gamma_t \approx 10^{-25} \text{ s} < 1/\Lambda_{\text{QCD}} \approx 10^{-24} \text{ s} < m_t / \Lambda_{\text{QCD}}^2 \approx 10^{-21} \text{ s} \ll \tau_b$$

decay

hadronization

spin decorrelation

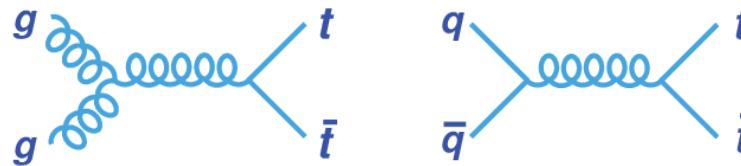


Decays before hadronising → access to bare quark properties

Spin information preserved → can measure its quantum state

Leptons and *d*-type quark (from *W*)
for maximal top quark spin transfer:
 α (spin analyzing power) → 1

In top quark pair production (*tt*):



top-antitop spins stay correlated (two qubit system)

- inferred from the decay products' angular distributions
- **polarization and spin correlation measurements** already in LHC Run-1 & Tevatron
- recently also **tests Quantum Theory with unstable particles (quarks)** at **high energies** in **specific phase regions**

Entangled particles → their quantum state cannot be described independently !

Top quark spin density matrix

Mixed states described in terms of the density matrix: $\rho = \sum_i p_i |\psi_i\rangle \langle \psi_i|$ Probability of being in state i

The top quark spin density matrix has decomposition:

$$\rho = \left(\mathbb{1}_4 + \sum_{i=1}^3 \left[B_i^+ \sigma^i \otimes \mathbb{1}_2 + B_i^- \mathbb{1}_2 \otimes \sigma^i \right] + \sum_{i,j=1}^3 C_{ij} \sigma^i \otimes \sigma^j \right) / 4$$

Spin polarisations
Spin correlation matrix

Spin dependence of $t\bar{t}$ production is completely characterized by 15 coefficients

Probed by angular distribution of decay products (spin analyzers)

Double diff. xsec

Polarisation (0 in SM)

Spin Correlation

$$\frac{1}{\sigma} \frac{d^2\sigma}{d\cos\theta_+^a d\cos\theta_-^b} = \frac{1}{4} (1 + B_+^a \cos\theta_+^a + B_-^b \cos\theta_-^b - C(a,b) \cos\theta_+^a \cos\theta_-^b)$$

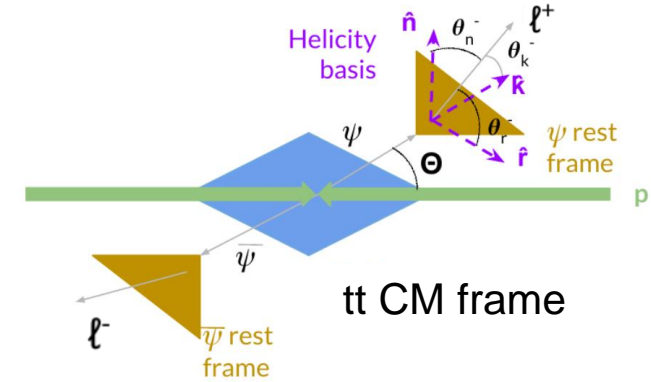
For each of the coefficients, a change of variables can be made to obtain a single differential cross section that depends only on that coefficient.

$$B^i = 3 \langle \cos\theta^i \rangle$$

$$C_{ij} = -9 \langle \cos\theta_1^i \cos\theta_2^j \rangle$$

Top polarisation and spin correlations

Each element of the spin density matrix can be probed through a unique angular distribution measured in helicity bases $\{\hat{k}, \hat{r}, \hat{n}\}$ (defined in the parent particle frame)



Observable	Measured coefficient	Symmetries
$\cos \theta_1^k$	B_1^k	P -odd, CP -even
$\cos \theta_2^k$	B_2^k	P -odd, CP -even
$\cos \theta_1^r$	B_1^r	P -odd, CP -even
$\cos \theta_2^r$	B_2^r	P -odd, CP -even
$\cos \theta_1^n$	B_1^n	P -even, CP -even
$\cos \theta_2^n$	B_2^n	P -even, CP -even
$\cos \theta_1^{k*}$	B_1^{k*}	P -odd, CP -even
$\cos \theta_2^{k*}$	B_2^{k*}	P -odd, CP -even
$\cos \theta_1^{r*}$	B_1^{r*}	P -odd, CP -even
$\cos \theta_2^{r*}$	B_2^{r*}	P -odd, CP -even
$\cos \theta_1^k \cos \theta_2^k$	C_{kk}	P -even, CP -even
$\cos \theta_1^r \cos \theta_2^r$	C_{rr}	P -even, CP -even
$\cos \theta_1^n \cos \theta_2^n$	C_{nn}	P -even, CP -even
$\cos \theta_1^r \cos \theta_2^k + \cos \theta_1^k \cos \theta_2^r$	$C_{rk} + C_{kr}$	P -even, CP -even
$\cos \theta_1^r \cos \theta_2^k - \cos \theta_1^k \cos \theta_2^r$	$C_{rk} - C_{kr}$	P -even, CP -odd
$\cos \theta_1^n \cos \theta_2^r + \cos \theta_1^r \cos \theta_2^n$	$C_{nr} + C_{rn}$	P -odd, CP -even
$\cos \theta_1^n \cos \theta_2^r - \cos \theta_1^r \cos \theta_2^n$	$C_{nr} - C_{rn}$	P -odd, CP -odd
$\cos \theta_1^n \cos \theta_2^k + \cos \theta_1^k \cos \theta_2^n$	$C_{nk} + C_{kn}$	P -odd, CP -even
$\cos \theta_1^n \cos \theta_2^k - \cos \theta_1^k \cos \theta_2^n$	$C_{nk} - C_{kn}$	P -odd, CP -odd

$$\frac{1}{\sigma} \frac{d\sigma}{d \cos \theta_1^i} = \frac{1}{2} (1 + B_1^i \cos \theta_1^i),$$

$$\frac{1}{\sigma} \frac{d\sigma}{d \cos \theta_2^i} = \frac{1}{2} (1 + B_2^i \cos \theta_2^i),$$

$$\frac{1}{\sigma} \frac{d\sigma}{dx} = \frac{1}{2} (1 - C_{ij} x) \ln \left(\frac{1}{|x|} \right),$$

$$x = \cos \theta_1^i \cos \theta_2^j.$$

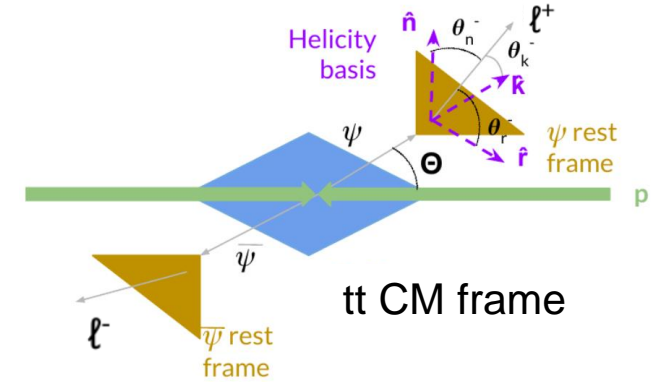
$$\frac{1}{\sigma} \frac{d\sigma}{dx_{\pm}} = \frac{1}{2} \left(1 - \frac{C_{ij} \pm C_{ji}}{2} x_{\pm} \right) \cos^{-1} |x_{\pm}|,$$

$$x_{\pm} = \cos \theta_1^i \cos \theta_2^j \pm \cos \theta_1^j \cos \theta_2^i.$$

off-diagonal redefined $C_{ij}^{\pm} = C_{ij} \pm C_{ji}$
only non-zero off-diagonal C_{rk}^{+}

Top polarisation and spin correlations

Each element of the spin density matrix can be probed through a unique angular distribution measured in helicity bases $\{\hat{k}, \hat{r}, \hat{n}\}$ (defined in the parent particle frame)



Observable	Measured coefficient	Symmetries
$\cos \theta_1^k$	B_1^k	P -odd, CP -even
$\cos \theta_2^k$	B_2^k	P -odd, CP -even
$\cos \theta_1^r$	B_1^r	P -odd, CP -even
$\cos \theta_2^r$	B_2^r	P -odd, CP -even
$\cos \theta_1^n$	B_1^n	P -even, CP -even
$\cos \theta_2^n$	B_2^n	P -even, CP -even
$\cos \theta_1^{k*}$	B_1^{k*}	P -odd, CP -even
$\cos \theta_2^{k*}$	B_2^{k*}	P -odd, CP -even
$\cos \theta_1^{r*}$	B_1^{r*}	P -odd, CP -even
$\cos \theta_2^{r*}$	B_2^{r*}	P -odd, CP -even
$\cos \theta_1^k \cos \theta_2^k$	C_{kk}	P -even, CP -even
$\cos \theta_1^r \cos \theta_2^r$	C_{rr}	P -even, CP -even
$\cos \theta_1^n \cos \theta_2^n$	C_{nn}	P -even, CP -even
$\cos \theta_1^r \cos \theta_2^k + \cos \theta_1^k \cos \theta_2^r$	$C_{rk} + C_{kr}$	P -even, CP -even
$\cos \theta_1^r \cos \theta_2^k - \cos \theta_1^k \cos \theta_2^r$	$C_{rk} - C_{kr}$	P -even, CP -odd
$\cos \theta_1^n \cos \theta_2^r + \cos \theta_1^r \cos \theta_2^n$	$C_{nr} + C_{rn}$	P -odd, CP -even
$\cos \theta_1^n \cos \theta_2^r - \cos \theta_1^r \cos \theta_2^n$	$C_{nr} - C_{rn}$	P -odd, CP -odd
$\cos \theta_1^n \cos \theta_2^k + \cos \theta_1^k \cos \theta_2^n$	$C_{nk} + C_{kn}$	P -odd, CP -even
$\cos \theta_1^n \cos \theta_2^k - \cos \theta_1^k \cos \theta_2^n$	$C_{nk} - C_{kn}$	P -odd, CP -odd

→ Measured with Run-1 data

$$\frac{1}{\sigma} \frac{d\sigma}{d \cos \theta_1^i} = \frac{1}{2} (1 + B_1^i \cos \theta_1^i),$$

$$\frac{1}{\sigma} \frac{d\sigma}{d \cos \theta_2^j} = \frac{1}{2} (1 + B_2^j \cos \theta_2^j),$$

$$\frac{1}{\sigma} \frac{d\sigma}{dx} = \frac{1}{2} (1 - C_{ij} x) \ln \left(\frac{1}{|x|} \right),$$

$$x = \cos \theta_1^i \cos \theta_2^j.$$

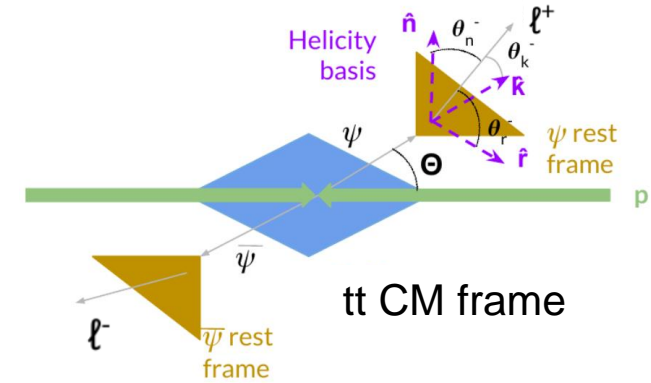
$$\frac{1}{\sigma} \frac{d\sigma}{dx_{\pm}} = \frac{1}{2} \left(1 - \frac{C_{ij} \pm C_{ji}}{2} x_{\pm} \right) \cos^{-1} |x_{\pm}|,$$

$$x_{\pm} = \cos \theta_1^i \cos \theta_2^j \pm \cos \theta_1^j \cos \theta_2^i.$$

off-diagonal redefined $C_{ij}^{\pm} = C_{ij} \pm C_{ji}$
only non-zero off-diagonal C_{rk}^{+}

Top polarisation and spin correlations

Each element of the spin density matrix can be probed through a unique angular distribution measured in helicity bases $\{\hat{k}, \hat{r}, \hat{n}\}$ (defined in the parent particle frame)



Observable	Measured coefficient	Symmetries
$\cos \theta_1^k$	B_1^k	P -odd, CP -even
$\cos \theta_2^k$	B_2^k	P -odd, CP -even
$\cos \theta_1^r$	B_1^r	P -odd, CP -even
$\cos \theta_2^r$	B_2^r	P -odd, CP -even
$\cos \theta_1^n$	B_1^n	P -even, CP -even
$\cos \theta_2^n$	B_2^n	P -even, CP -even
$\cos \theta_1^{k*}$	B_1^{k*}	P -odd, CP -even
$\cos \theta_2^{k*}$	B_2^{k*}	P -odd, CP -even
$\cos \theta_1^{r*}$	B_1^{r*}	P -odd, CP -even
$\cos \theta_2^{r*}$	B_2^{r*}	P -odd, CP -even
$\cos \theta_1^k \cos \theta_2^k$	C_{kk}	P -even, CP -even
$\cos \theta_1^r \cos \theta_2^r$	C_{rr}	P -even, CP -even
$\cos \theta_1^n \cos \theta_2^n$	C_{nn}	P -even, CP -even
$\cos \theta_1^r \cos \theta_2^k + \cos \theta_1^k \cos \theta_2^r$	$C_{rk} + C_{kr}$	P -even, CP -even
$\cos \theta_1^r \cos \theta_2^k - \cos \theta_1^k \cos \theta_2^r$	$C_{rk} - C_{kr}$	P -even, CP -odd
$\cos \theta_1^n \cos \theta_2^r + \cos \theta_1^r \cos \theta_2^n$	$C_{nr} + C_{rn}$	P -odd, CP -even
$\cos \theta_1^n \cos \theta_2^r - \cos \theta_1^r \cos \theta_2^n$	$C_{nr} - C_{rn}$	P -odd, CP -odd
$\cos \theta_1^n \cos \theta_2^k + \cos \theta_1^k \cos \theta_2^n$	$C_{nk} + C_{kn}$	P -odd, CP -even
$\cos \theta_1^n \cos \theta_2^k - \cos \theta_1^k \cos \theta_2^n$	$C_{nk} - C_{kn}$	P -odd, CP -odd
$\cos \varphi$	D	P -even, CP -even

→ Measured with Run-1 data

$$D = -\text{Tr}[C]/3 = -(C_{kk} + C_{rr} + C_{nn})/3.$$

$D \neq 0$ top quark spins are correlated

Conditions for quantum entanglement

(based on Peres-Horodecki criterion)

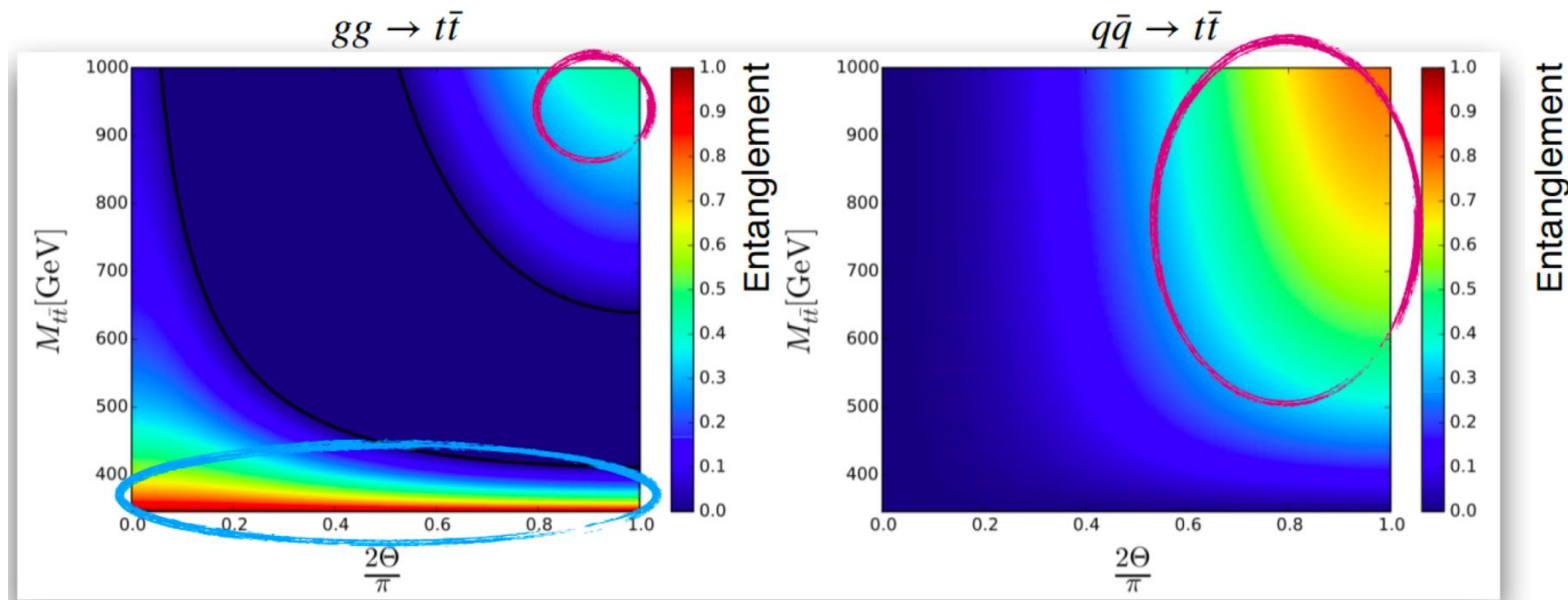
$$\Delta \equiv -C_{nn} + |C_{kk} + C_{rr}| - 1 > 0$$

$$D = -\frac{(C_{kk} + C_{rr} + C_{nn})}{3} < -1/3$$

$$D_n = \tilde{D} = \frac{(C_{kk} + C_{rr} - C_{nn})}{3} < -1/3$$

In $t\bar{t}$ production, the SM predicts entangled states:

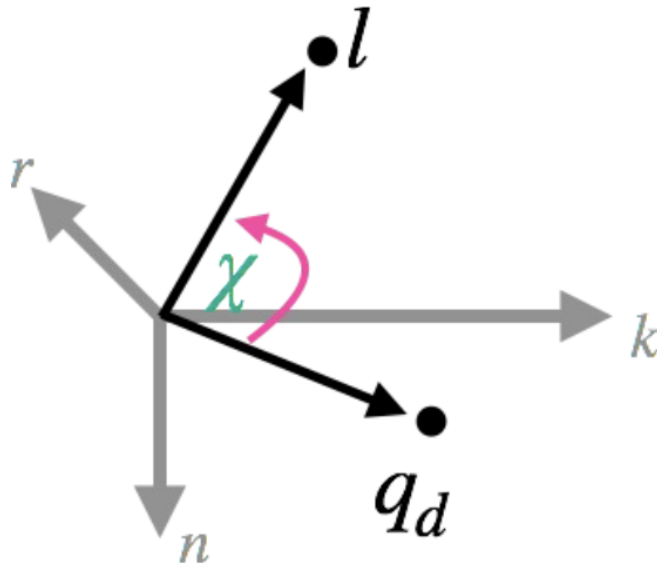
- at the production threshold region in gg -fusion production
- at the boosted region for central production of the system



Eur. Phys. J. Plus (2021) 136:907 (Afik, De Nova)

Sensitive observables to entanglement with top quarks

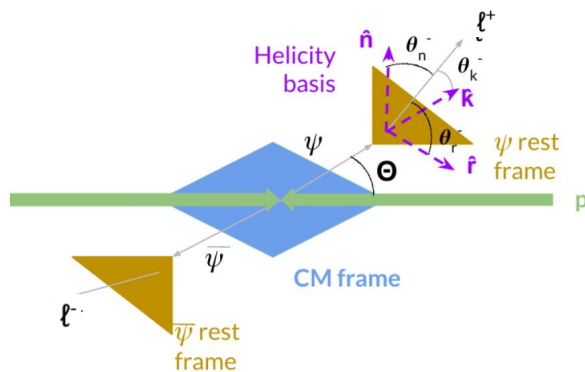
Remarkably entanglement can also be probed from single differential distributions



Threshold

$$\frac{d\sigma}{d\cos\chi} = A(1 + D\kappa\bar{\kappa}\cos\chi)$$

angle between the directions of two decay products measured in their parent top quark and antiquark rest frames



Boosted

$$\frac{d\sigma}{d\cos\tilde{\chi}} = A(1 + \tilde{D}\kappa\bar{\kappa}\cos\tilde{\chi})$$

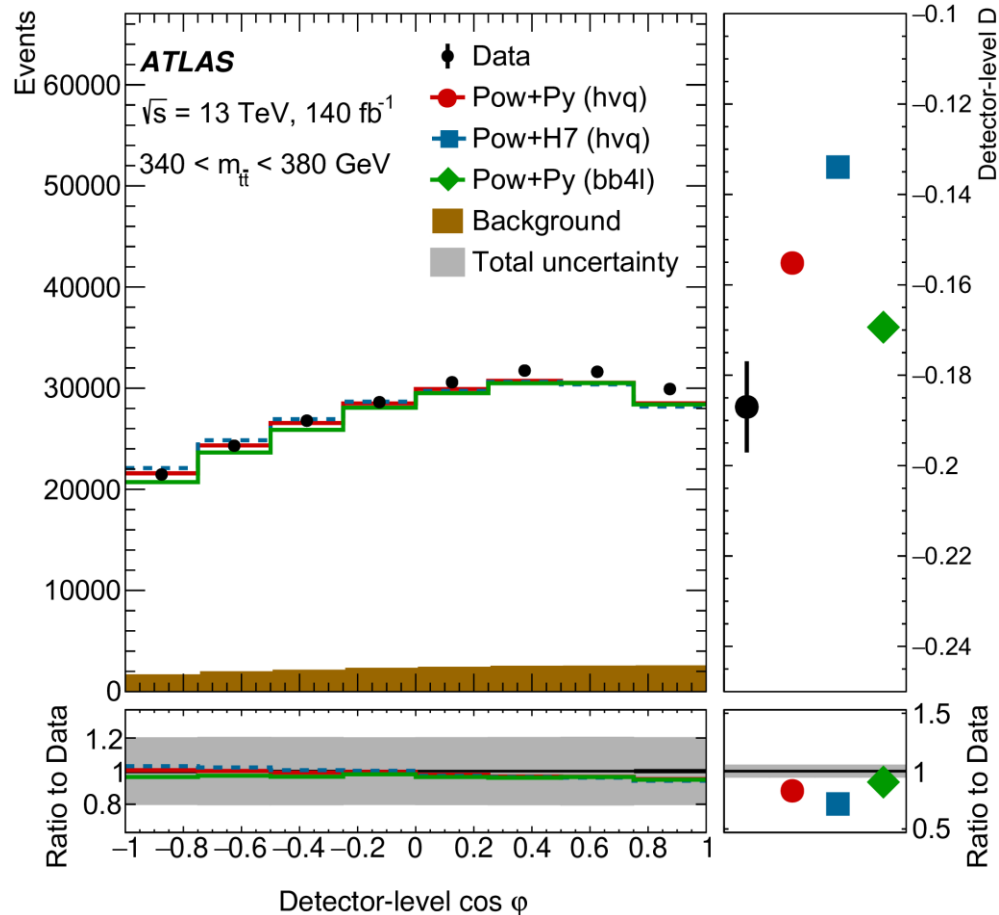
with inverted sign of n-component in one of the decay products

ATLAS: 1st observation of entanglement in top quarks

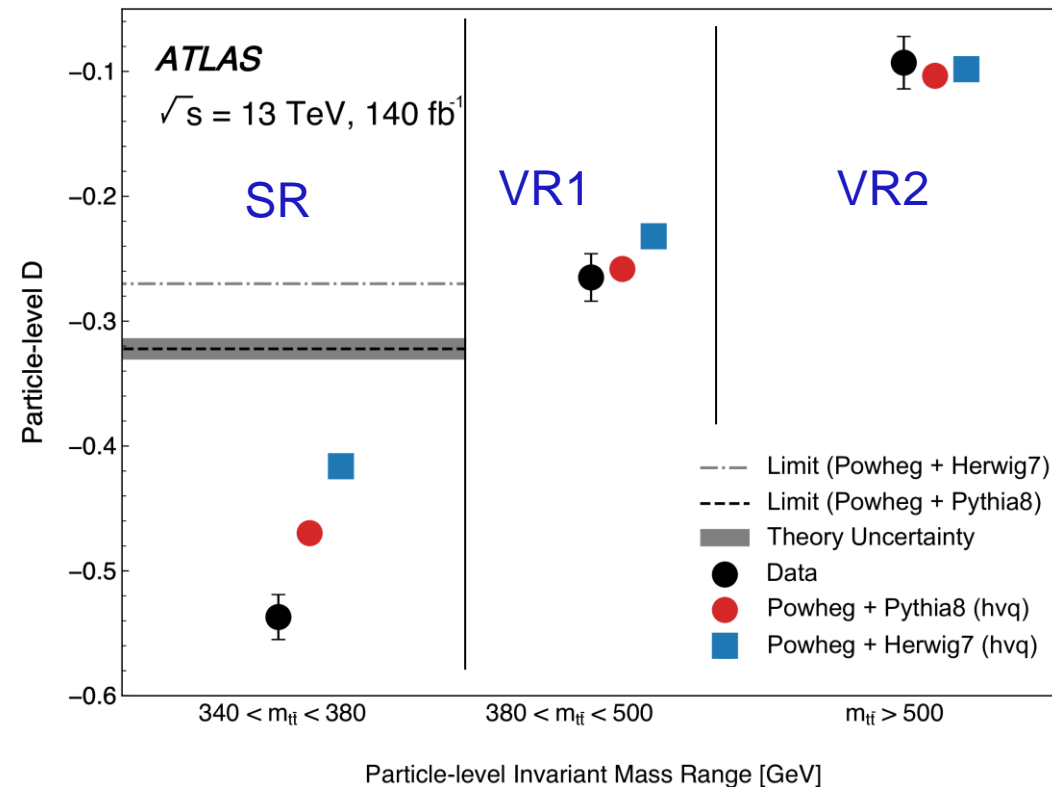
Nature 633 (2024) 542

- Focus on the threshold region, $m_{t\bar{t}} < 380$ GeV
- Using dilepton $e\mu$ channel, ≥ 2 jets, ≥ 1 b-jet (85% eff.)
- Top reconstruction: ellipse method for neutrino reco.
- Nominal signal model: Powheg+Py8
- Results quoted at particle-level

Detector-level



Particle-level results in SR and VRs



Data few sigmas away from MC expectation in SR ...
Agreement in the validation regions

First observation of entanglement with significance $> 5\sigma$
Leading unc. is parton shower modelling

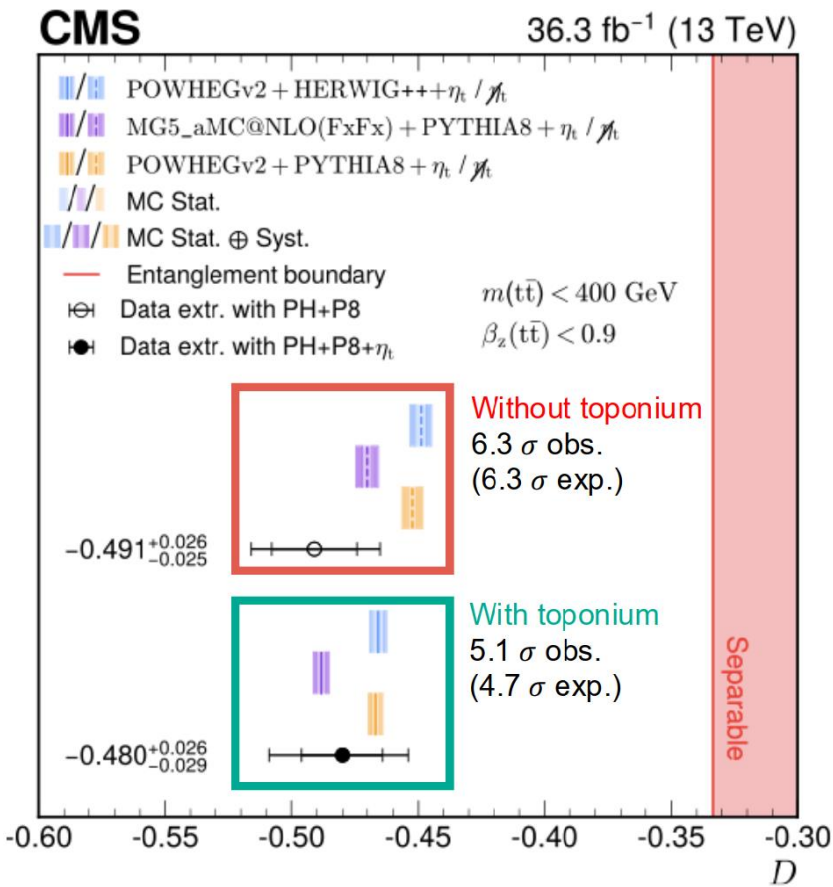
CMS threshold results using dilepton channel

Rep. Prog. Phys 87 (2024) 117801

- Partial Run-2 dataset; $e\mu+ee+\mu\mu$ channels, ≥ 2 jets, ≥ 1 b -jet
- Focus on low-mass region ($345 < m_{t\bar{t}} < 400$ GeV)
- Cut on velocity of the $t\bar{t}$ system ($\beta < 0.9$) to increase fraction of gg events
- Kinematic top reconstructed (weighting method)
- Includes toponium model with MG5_aMC@NLO (LO) + Py8
- D extracted at parton-level from binned profile likelihood fit to angular distribution

Toponium simulated as a pseudo-scalar color singlet and spin-0 particle with $m=343$ GeV and $\sigma=6.4$ pb

5 σ observation of top quarks entangled at threshold
Agreement with SM significantly improved by including η_t
 $\sim 1.5\sigma$ tension with the expectation without η_t



Source	Uncertainty
	$D_{345 < m_{t\bar{t}} < 400}$
Toponium normalization	9.79%
JES	9.68%
Parton Shower (ISR)	6.81%
Scale	1.68%
Parton Shower (FSR)	1.00%
JER	0.76%
Z+jets shape	0.67%
Top quark p_T	0.23%
PDF	0.16%
Color reconnection	0.11%

CMS lepton+jets channel: strategy

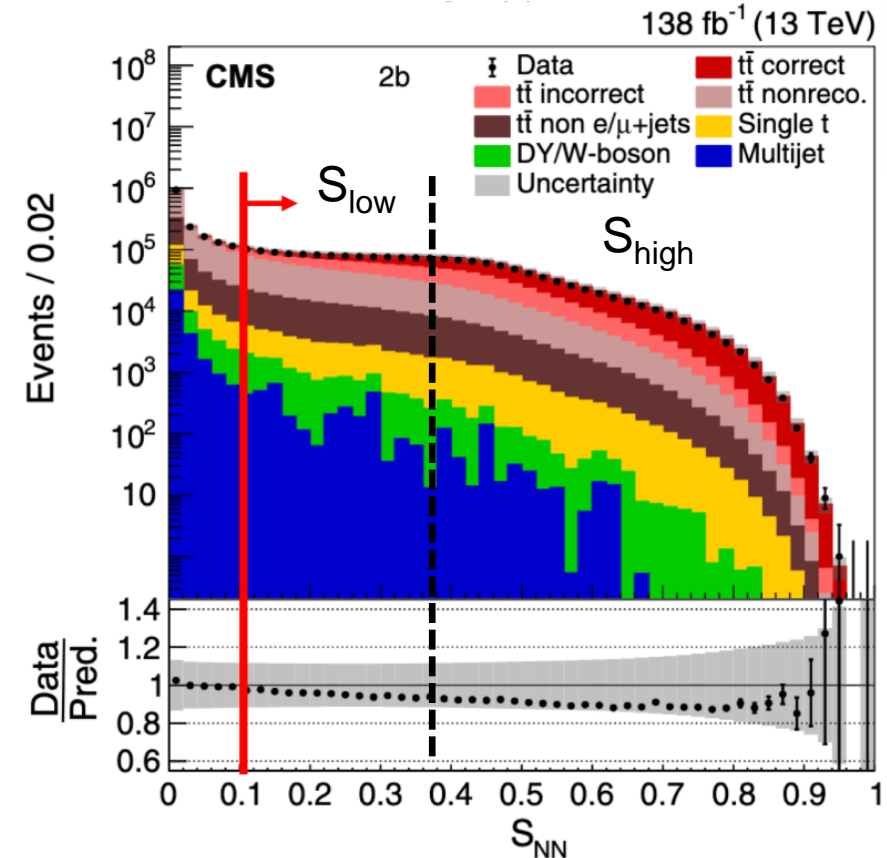
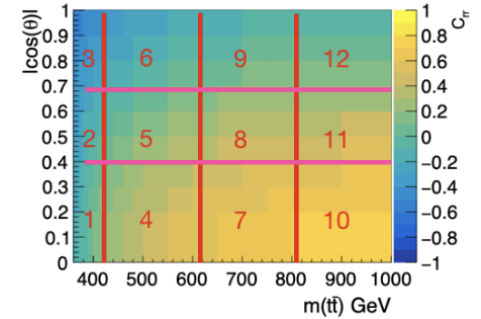
Phys. Rev. D 110 (2024) 112016

- Evaluation of full correlation matrix C and polarization vectors B , as well as ΔE , D & D_n
Inclusive + differential measurements in bins of $m_{tt}/p_{T,t}$ and $\cos(\theta)$
- Nominal signal: Powheg+Py8+EWK corr. from HATHOR
(higher order QCD unc. from Powheg MiNNLO)
- Challenging identification of d -type quark in W decay
- NN used to reco tt system, with inputs: lepton and jet kinematics, b -tagging scores & $E_{T,miss}$
Reduce bkg. by mass window cuts in top and W mass
Remove events with $S_{NN} < 0.1$
- 4 event categories based on # b -tags & S_{NN} score

$$\begin{aligned} S_{\text{low}}(1b): S_{NN} < 0.30 & \quad S_{\text{high}}(1b): S_{NN} \geq 0.30 \\ S_{\text{low}}(2b): S_{NN} < 0.36 & \quad S_{\text{high}}(2b): S_{NN} \geq 0.36 \end{aligned}$$

optimized to minimize unc. in spin density matrix

Reco efficiency of the NN (including d -type id):
40% for $S_{\text{low}}(1b)$ - 75% for $S_{\text{high}}(2b)$



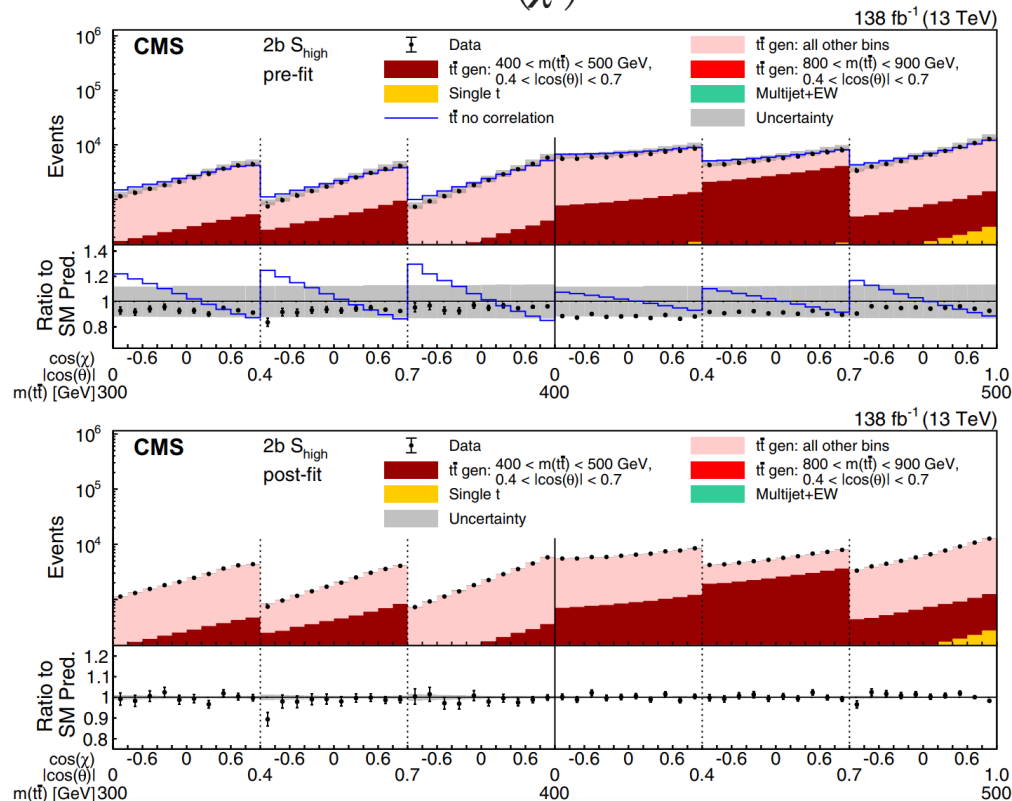
CMS lepton+jets channel: fits to various distributions

Binned maximum likelihood fit combining information of the 4 categories of various distributions in various regions of phase space - bins of $m_{t\bar{t}}/p_{T,t}$ and $\cos(\theta)$ -

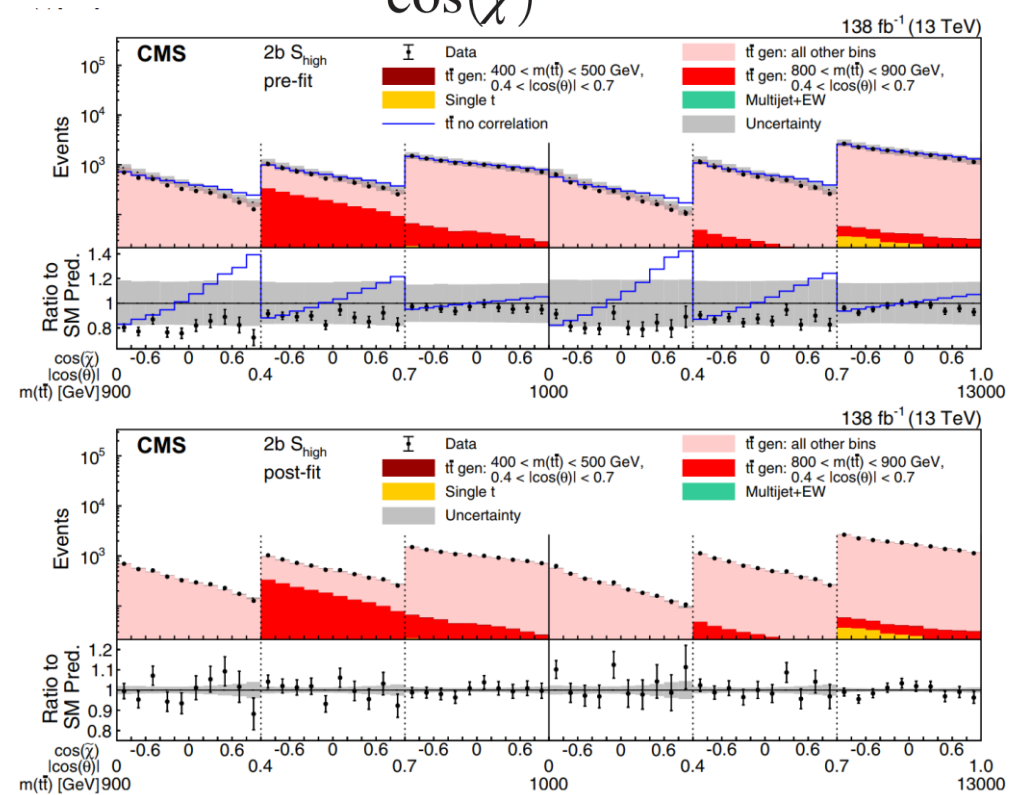
- unrolled 4D distribution of $\phi_{\bar{p}}, \cos(\theta_{\bar{p}}), \phi_p$, and $\cos(\theta_p) \rightarrow$ to extract full matrix coefficients
- $\cos(\chi)$ and $\cos(\tilde{\chi})$ distribution \rightarrow to study quantum entanglement

to reco-level templates (one for each coefficient)

$\cos(\chi)$



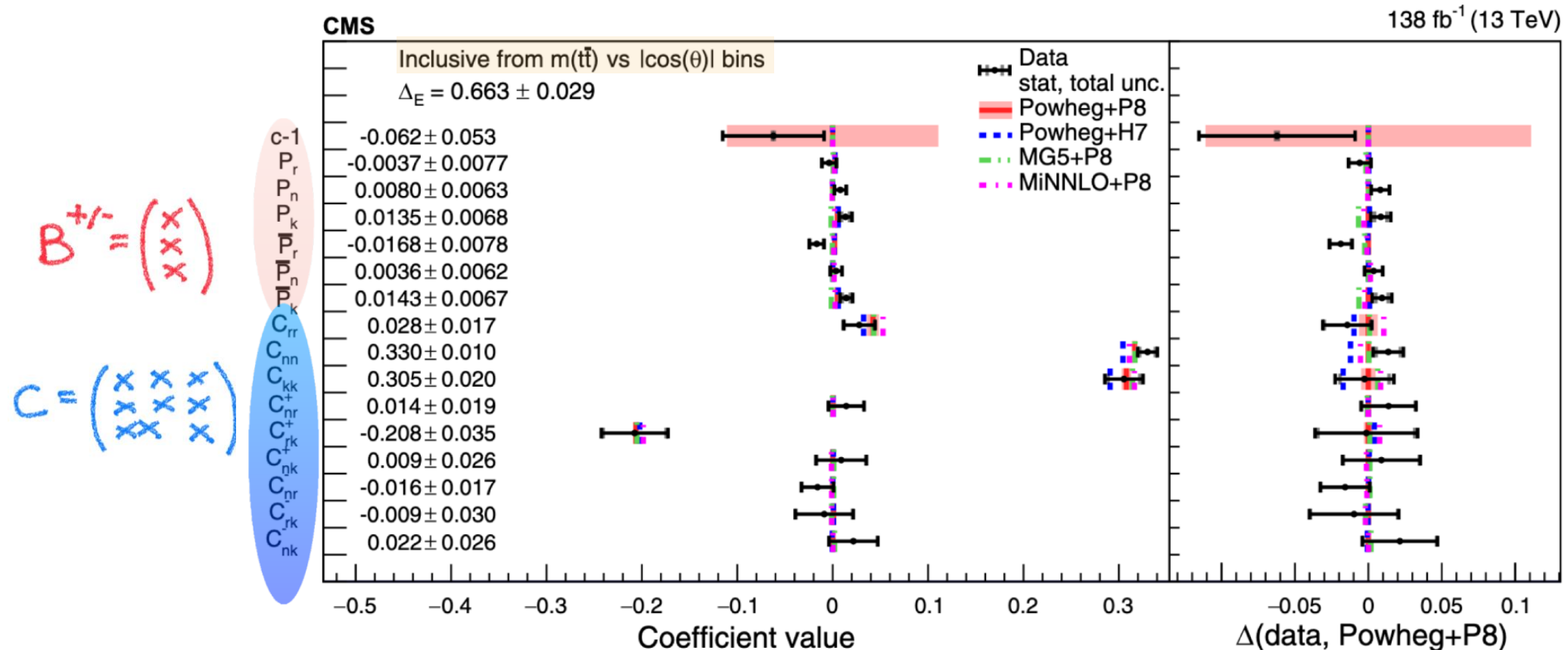
$\cos(\tilde{\chi})$



CMS l+jets: polarisation vectors & spin corr. matrix coef.

Phys. Rev. D 110 (2024) 112016

Full measurement of the polarisation vector and coefficients of the spin correlation matrix performed inclusively and differentially in bins of $m_{tt} \times \cos(\theta)$ or $p_{T,t} \times \cos(\theta)$

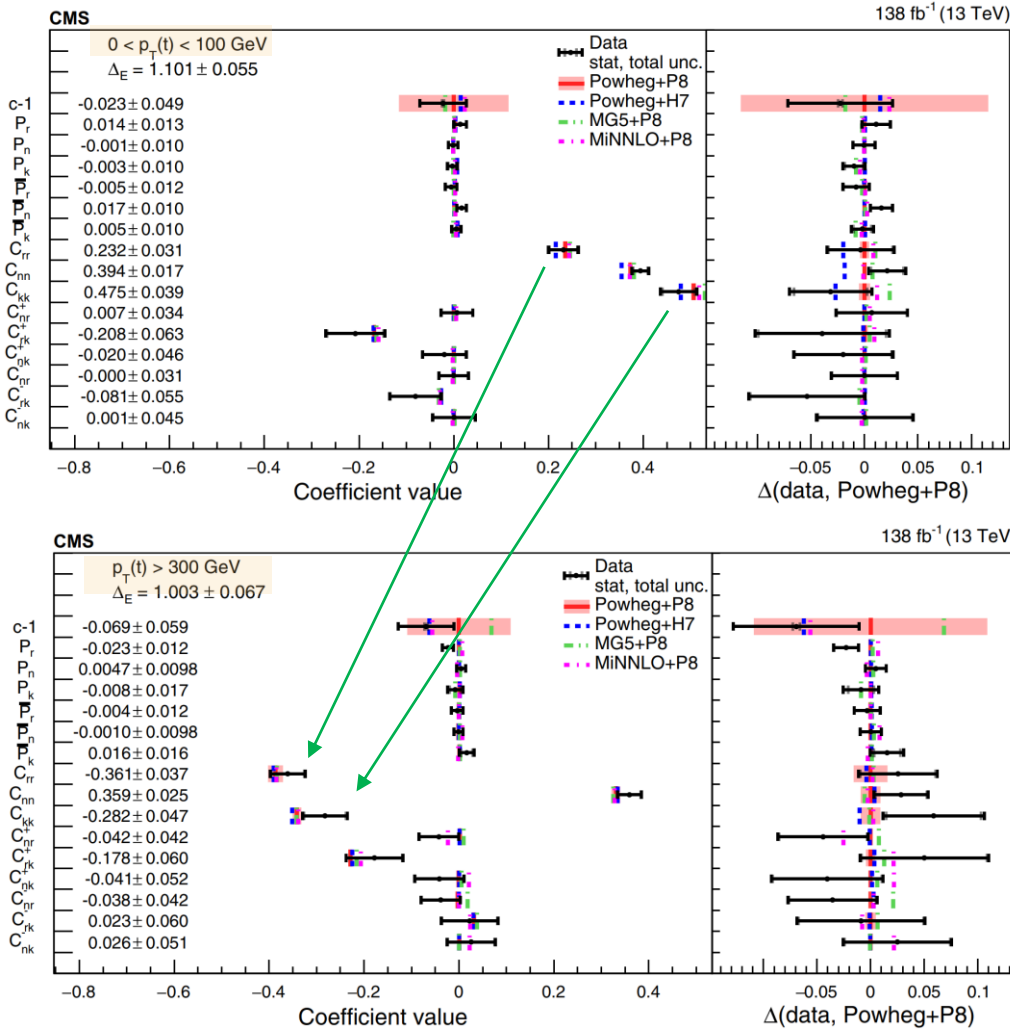


off-diagonal redefined $C_{ij}^{\pm} = C_{ij} \pm C_{ji}$

- Only C_{rk}^+ is invariant under P and CP parity transformation and is the only non-zero off-diagonal element
- Good agreement wrt. SM and previous results

CMS l+jets: polarisation vectors & spin corr. matrix coef.

Phys. Rev. D 110 (2024) 112016

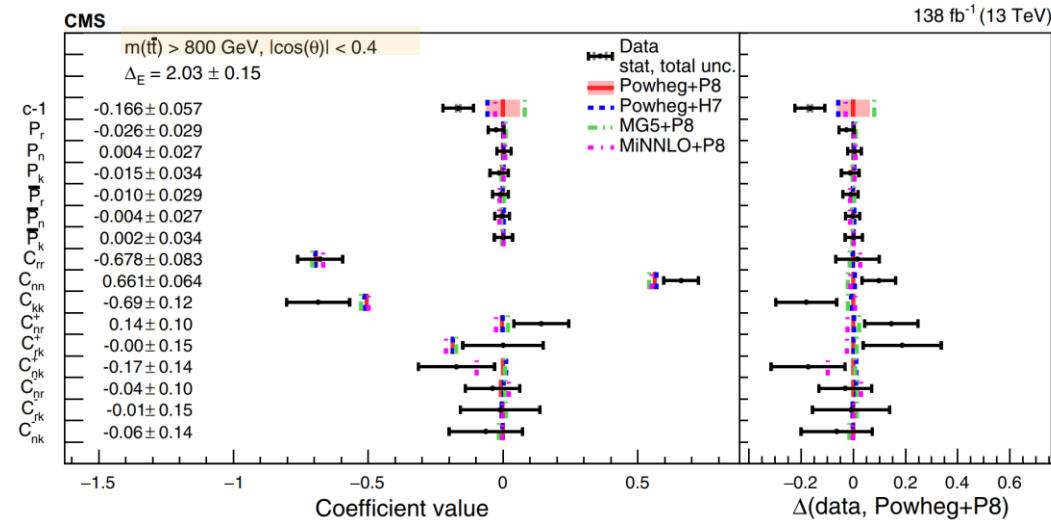


- With these measurements, the differences in the spin correlation for various kinematic regions become clearly visible
- For the $p_{T,t}$ measurement, the signs of C_{rr} and C_{kk} change from positive to negative with increasing $p_{T,t}$
- Diagonal elements indicate the transition from the spin-singlet to the spin-triplet as the dominant state

$$C_{nn}, C_{rr}, C_{kk} > 0$$

$$C_{nn} > 0$$

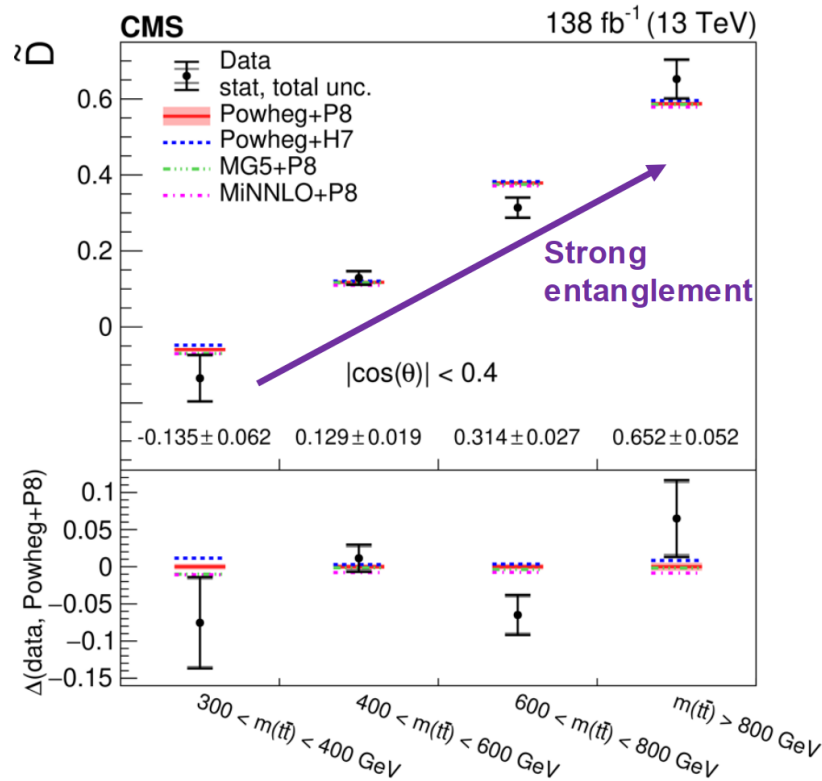
$$C_{rr}, C_{kk} < 0$$



First at high m_{tt}

CMS lepton+jets channel: quantum entanglement

Phys. Rev. D 110 (2024) 112016

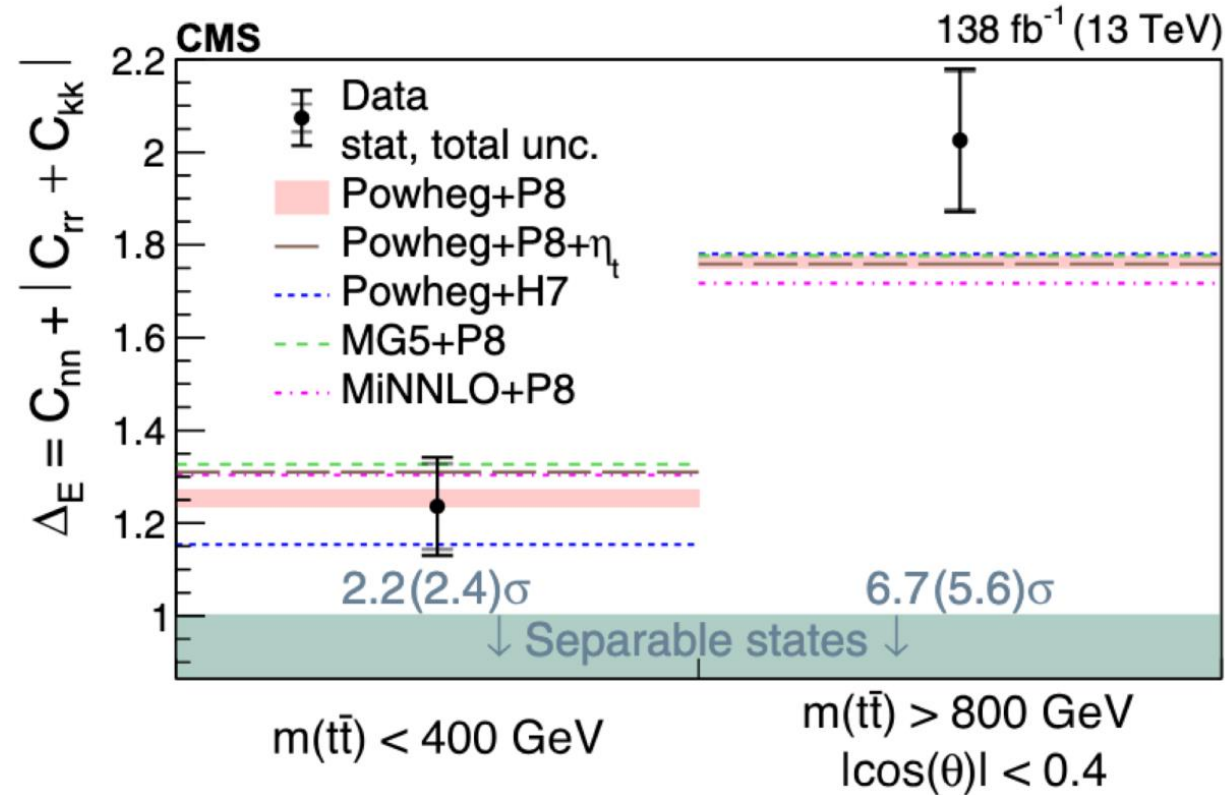


Good agreement with predictions

- Entanglement observed for first time in events with high $m_{t\bar{t}}$!

highest sensitivity using full matrix C

- No sensitivity in low $m_{t\bar{t}}$ region



Evaluation of “magic” states of the tt system (CMS)

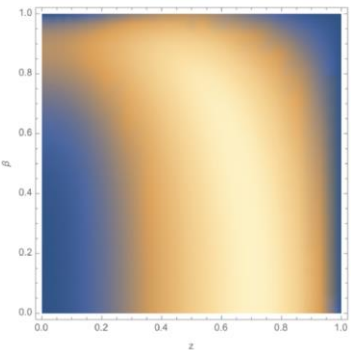
CMS PAS TOP-25-001

- “Quantum Magic” quantifies computational advantage of quantum over classical states
 - Entanglement by itself doesn’t guarantee this
- For mixed states:

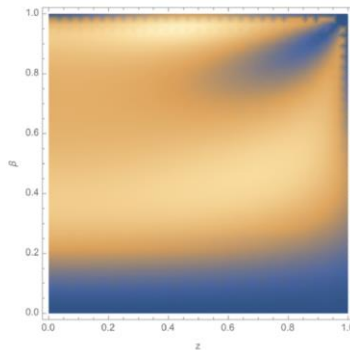
$$\tilde{M}_2 = -\log_2 \left(\frac{1 + \sum_{i \in n, k, r} [(P_i^4 + \bar{P}_i^4)] + \sum_{i, j \in n, k, r} C_{ij}^4}{1 + \sum_{i \in n, k, r} [(P_i^2 + \bar{P}_i^2)] + \sum_{i, j \in n, k, r} C_{ij}^2} \right)$$

can be calculated from the measured 15 coefficients

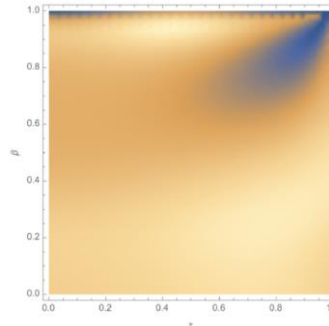
$q\bar{q}$



gg

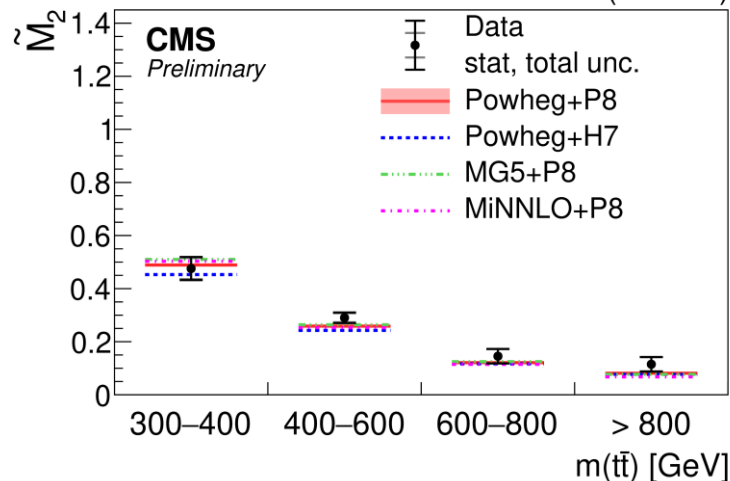


pp

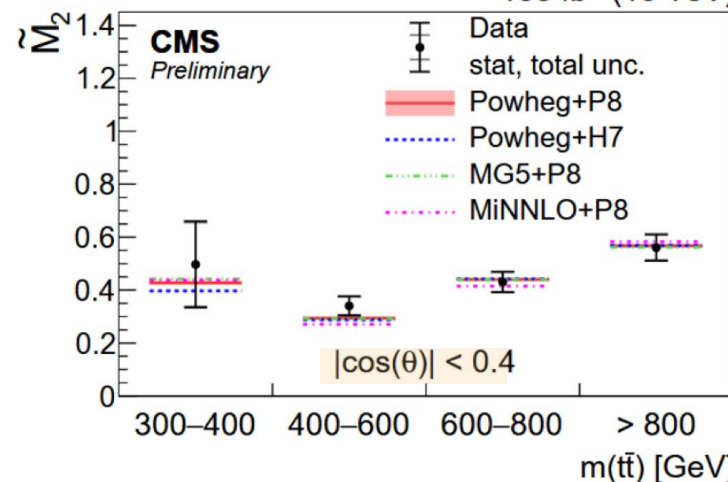


- M_2 is phase-space dependent
- For $pp \rightarrow t\bar{t}$: M_2 maximal near threshold

138 fb⁻¹ (13 TeV)



138 fb⁻¹ (13 TeV)



- Flat after a cut on $\cos(\theta)$
- In agreement with the SM
- Limited by stat unc.

- Assumptions made:

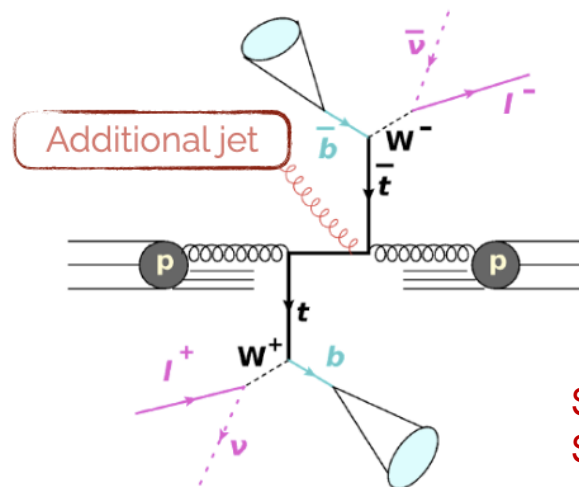
- angular distribution of decay products gives direct access to the top spin polarization
- NLO corrections in $t\bar{t}$ entanglement are small

→ Need to revisit these if we plan to carry out high-precision measurements of spin entanglement at LHC

Ex.: if new physics modifies the *spin-analyzing power* α , the measured observables would be biased

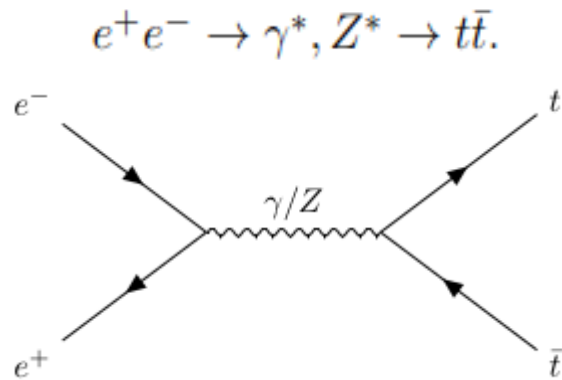
- The quantum systems that we have studied (top quarks) decay and interact...

→ **Understanding spin decoherence (loss of information) from final-state radiation is a critical challenge** in this new frontier in HEP that connects quantum information science and collider physics...



Sketch from
Sebastian Wuchterl

Can we study quantum decoherence at colliders?



Pheno study (work in progress):

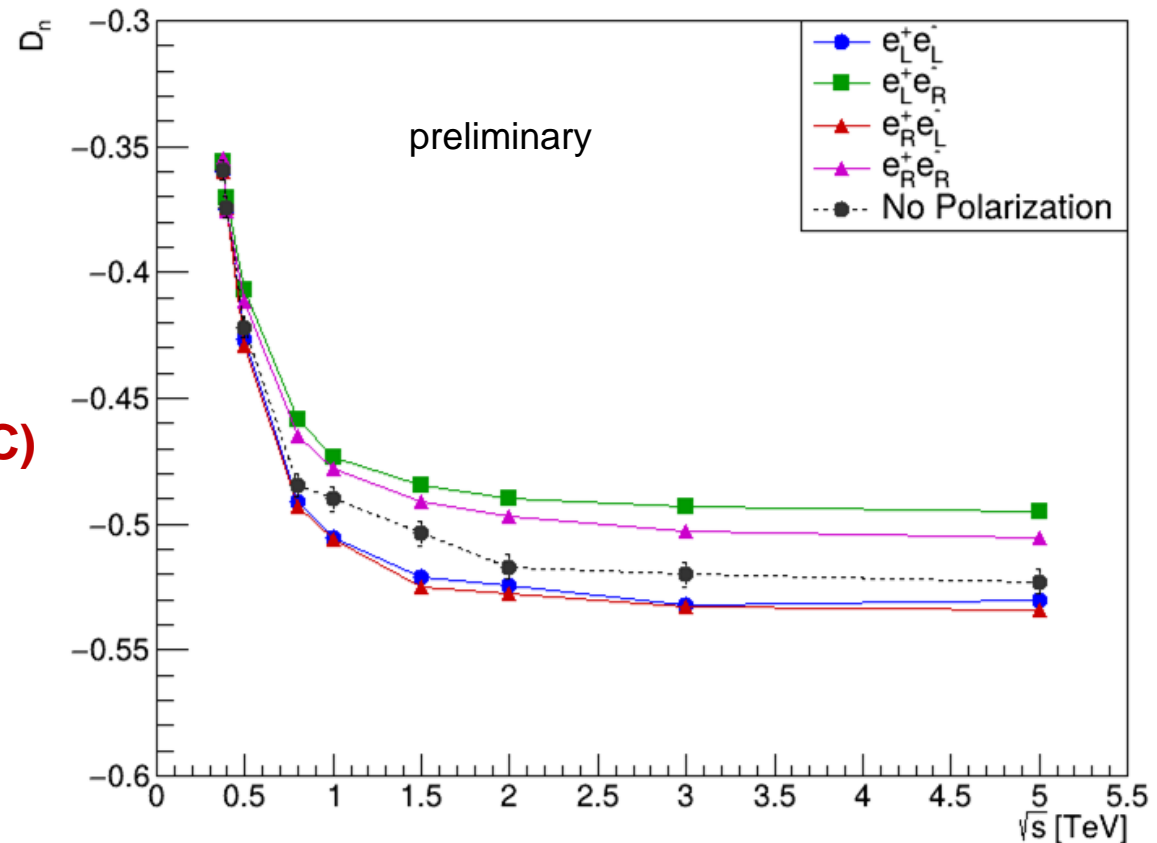
- simulations $e^+e^- \rightarrow t\bar{t}$ at various \sqrt{s}
- assumed int. lumi. 8 ab^{-1} (LCF)
- $(P_{e^+}, P_{e^-}) = (\pm 30\%, \pm 80\%)$

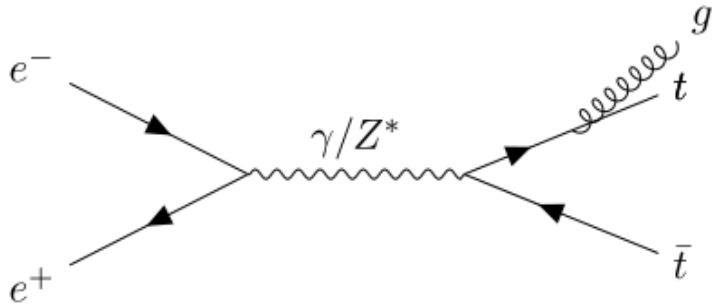
Quantum entanglement using D_n (and C)

- $D_n < -\frac{1}{3}$ & $> 5\sigma$ observation for all \sqrt{s}
- Entanglement increases with \sqrt{s}
- Degree of entanglement changes with the initial polarization of the beams

Very difficult at the LHC...

but we can explore this in cleaner environments such as lepton colliders ☺



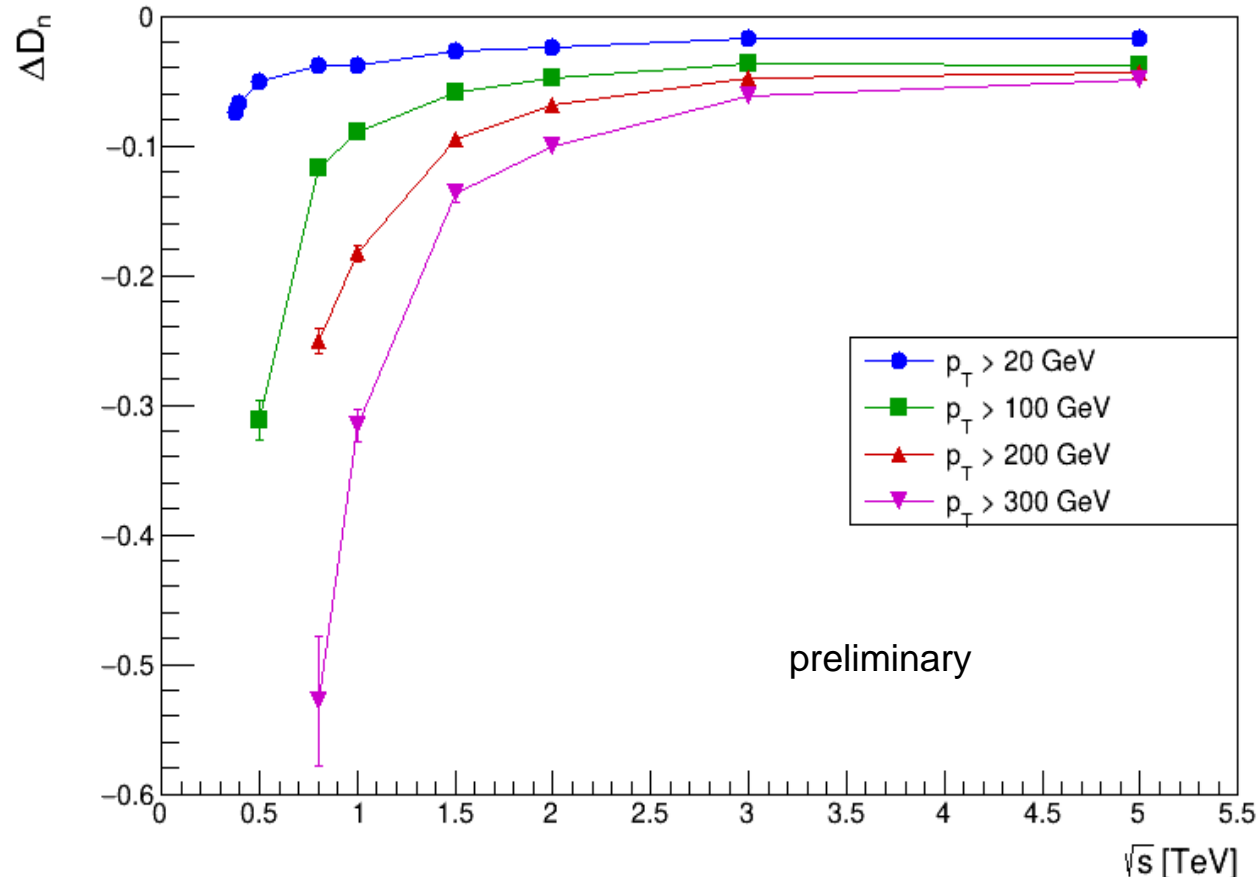


simulations $e^+e^- \rightarrow ttg$ at various \sqrt{s}

$D_n(ttg) < D_n(tt)$
 Decoherence effects are stronger
 when the gluon is more energetic

Same behaviour observed for ΔR ,
 but with a less pronounced
 decoherence effect

$$\Delta D_n = D_n^{t\bar{t}} - D_n^{t\bar{t}g} \quad \text{for various gluon } p_T \text{ cuts and } \sqrt{s}$$



Gluon decoherence study: D_n

\sqrt{s}

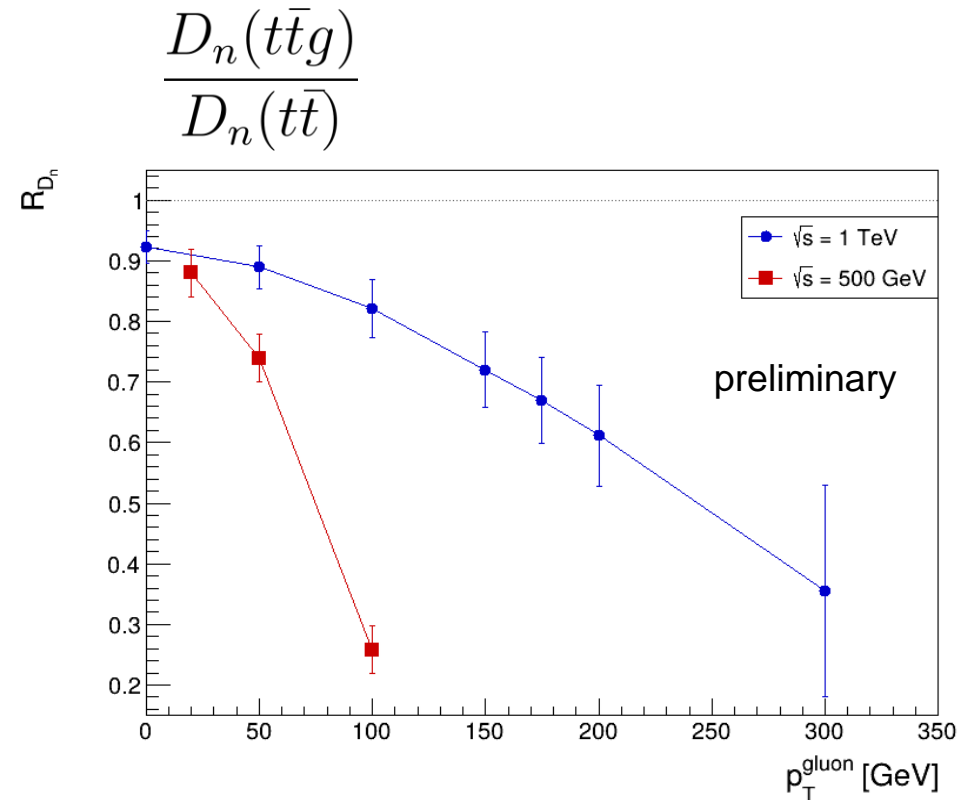
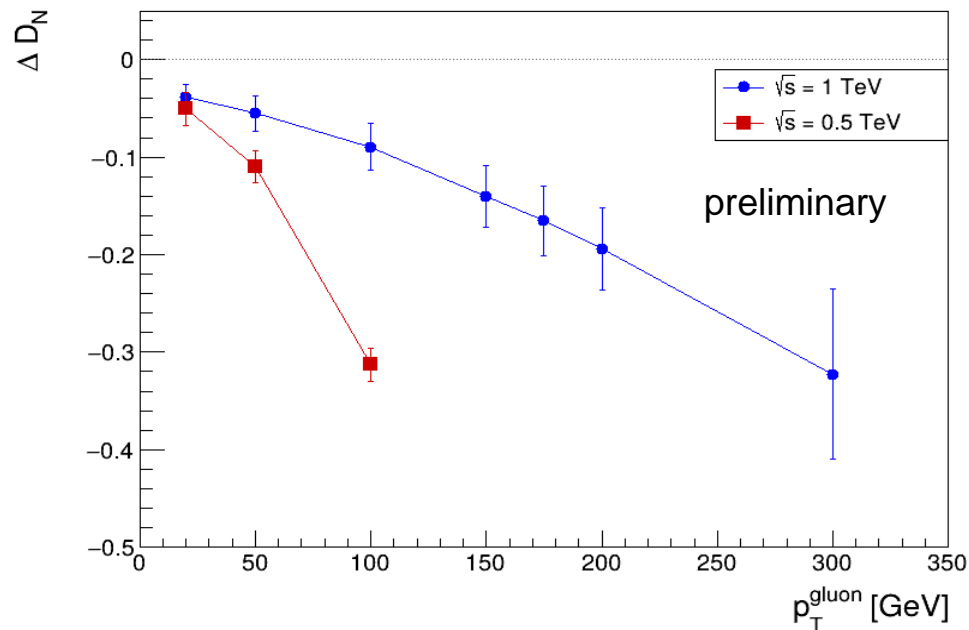
500 GeV

1 TeV

Final State	$t\bar{t}$	$D_n: e^+e^- \rightarrow t\bar{t}g$	ΔD_n ($t\bar{t} - t\bar{t}g$)	significance ($\Delta D_n > 0$)	$R_{D_n} = D_n^{t\bar{t}g}/D_n^{t\bar{t}}$	significance ($R_{D_n} < 1$)
ee, $\mu\mu$, $e\mu$	-0.4217 ± 0.0037	-0.371 ± 0.017 ($p_T > 20\text{GeV}$)	-0.050 ± 0.017	3.0σ	0.881 ± 0.039	3.0σ
ee, $\mu\mu$, $e\mu$ & e/μ +jets	idem. ± 0.0017	idem. ± 0.0074	idem. ± 0.0076	6.6σ	idem. ± 0.018	6.6σ
all channels	idem. ± 0.00075	idem. ± 0.0032	idem. ± 0.0033	15σ	idem. ± 0.0078	15σ
ee, $\mu\mu$, $e\mu$	-0.5004 ± 0.0067	-0.360 ± 0.031 ($p_T > 150\text{GeV}$)	-0.140 ± 0.032	4.4σ	0.720 ± 0.063	4.5σ
ee, $\mu\mu$, $e\mu$ & e/μ +jets	idem. ± 0.0031	idem. ± 0.014	idem. ± 0.015	9.6σ	idem. ± 0.028	9.8σ
all channels	idem. ± 0.0014	idem. ± 0.0062	idem. ± 0.0063	22σ	idem. ± 0.013	22σ

Could observe decoherence effect at future lepton colliders !

$$\Delta D_n = D_n^{t\bar{t}} - D_n^{t\bar{t}g}$$



Gluon decoherence study: concurrence $\mathcal{C}(\rho)$

Definition of concurrence for a mixed state of two qubits:

$$\mathcal{C}(\rho) \equiv \max(0, \lambda_1 - \lambda_2 - \lambda_3 - \lambda_4)$$

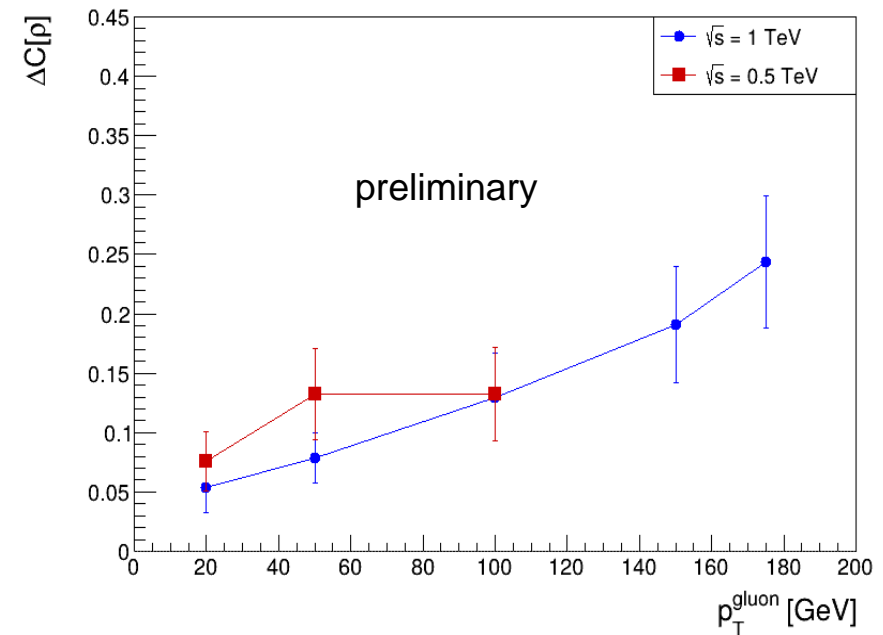
in which $\lambda_1, \dots, \lambda_4$ are the eigenvalues, in decreasing order, of the Hermitian matrix

$$R = \sqrt{\sqrt{\rho} \tilde{\rho} \sqrt{\rho}}$$

with

$$\tilde{\rho} = (\sigma_y \otimes \sigma_y) \rho^* (\sigma_y \otimes \sigma_y)$$

the spin-flipped state of ρ and σ_y a **Pauli spin matrix**. The



- More challenging experimentally!!
- Similar significance as for D_n
- Results to be validated with calculations (ongoing collaboration with R. Aoude, F. Maltoni and L. Satrioni)

30 years of top quark physics!

- $t\bar{t}$ spin correlation measurements in dilepton and lepton+jets channels in agreement with SM
 - Full spin-density matrix in the lepton+jets channel
 - First observations of entanglement between top quarks in top pair production at production threshold in dilepton ch. and boosted regime in lepton+jets ch.
 - Quantum magic measurement
 - one of the first connections between quantum information science and particle physics
 - shows the potential of collider experiments for testing foundations of quantum mechanics
- Studying decoherence effects is relevant and feasible in future lepton colliders using top quarks
 - Also prominent results using events with tau pairs from current Belle-2 experiment

$$e^+e^- \rightarrow \tau^+\tau^-\gamma$$

THANKS FOR YOUR ATTENTION



BACK-UP

Machine (LCF)	Final state	# $t\bar{t}$ events	# $t\bar{t}g$ events
$\sqrt{s} = 500$ GeV ($\int \mathcal{L} dt = 8 \text{ ab}^{-1}$) No polarization	ee, $\mu\mu$, $e\mu$ ee, $\mu\mu$, $e\mu$ & e/μ +jets all channels	$1.5 \cdot 10^6 \times 4\%$ $1.5 \cdot 10^6 \times 19^{*}\%$ $1.5 \cdot 10^6$	$0.5 \cdot 10^6 \times 4\%$ $0.5 \cdot 10^6 \times 19^{*}\%$ $0.5 \cdot 10^6$
$\sqrt{s} = 1$ TeV ($\int \mathcal{L} dt = 8 \text{ ab}^{-1}$) No polarization	ee, $\mu\mu$, $e\mu$ ee, $\mu\mu$, $e\mu$ & e/μ +jets all channels	$5 \cdot 10^6 \times 4\%$ $5 \cdot 10^6 \times 19^{*}\%$ $5 \cdot 10^6$	$0.3 \cdot 10^6 \times 4\%$ $0.3 \cdot 10^6 \times 19^{*}\%$ $0.3 \cdot 10^6$

($p_T > 20$ GeV)

($p_T > 150$ GeV)

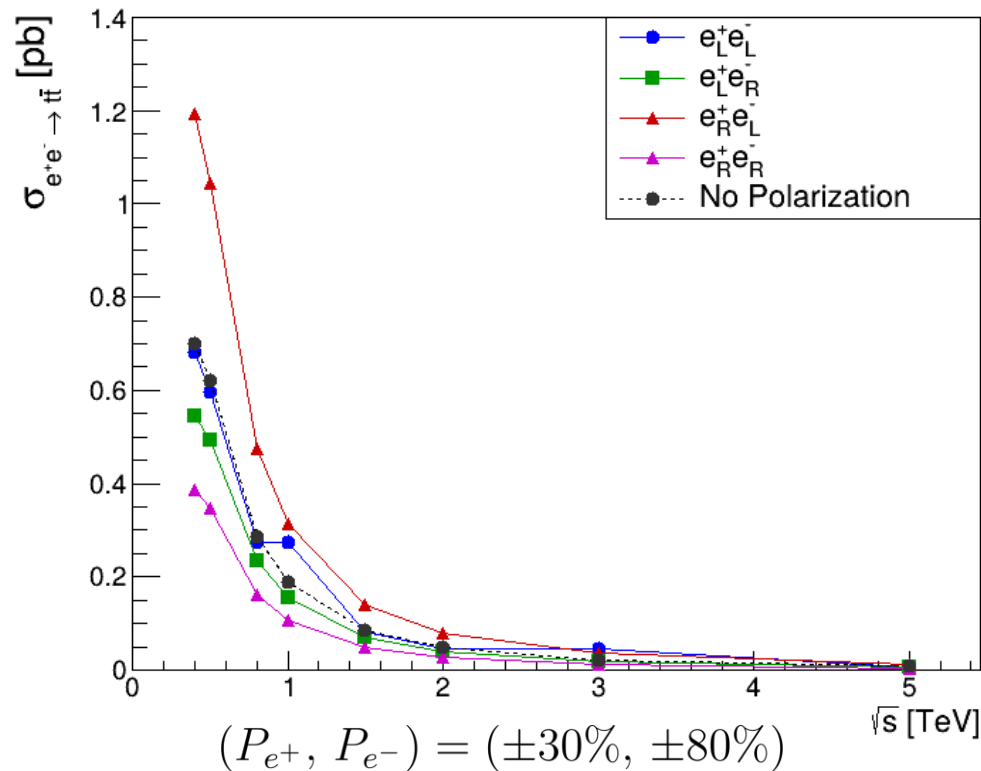
$$e^+e^- \rightarrow t\bar{t}$$

LCF

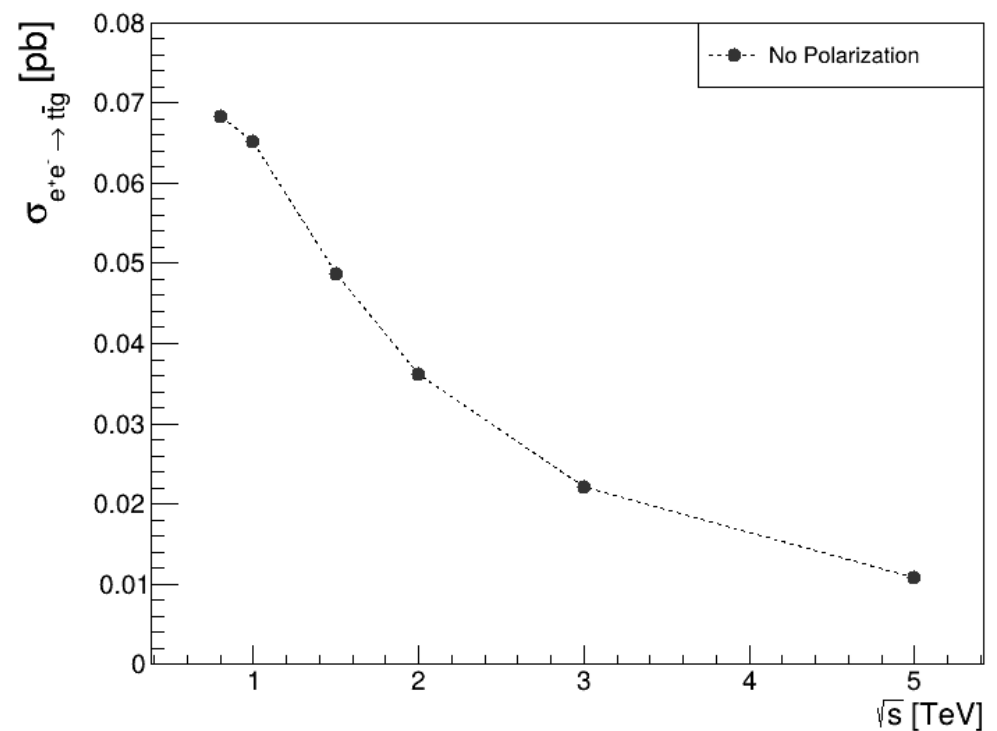
LCvision, arXiv: 2503.19983

	91 GeV	250 GeV	350 GeV	550 GeV	1-3 TeV
$\int \mathcal{L} \text{ (ab}^{-1}\text{)}$	0.1	3	0.4	8	8
beam polarisation (e^-, e^+ ; %)	80/30	80/30	80/30	80/60	80/20
($--, -+, +-, ++$) (%)	(10,40,40,10)	(5,45,45,5)	(5,68,22,5)	(10,40,40,10)	(10,40,40,10)

Without gluon radiation



With gluon radiation



Polarization basics

- Longitudinal polarization: $\mathcal{P} = \frac{N_R - N_L}{N_R + N_L}$

- Cross section:

$$\sigma(\mathcal{P}_{e-}, \mathcal{P}_{e+}) = \frac{1}{4} \{ (1 + \mathcal{P}_{e-})(1 + \mathcal{P}_{e+})\sigma_{RR} + (1 - \mathcal{P}_{e-})(1 - \mathcal{P}_{e+})\sigma_{LL} \\ + (1 + \mathcal{P}_{e-})(1 - \mathcal{P}_{e+})\sigma_{RL} + (1 - \mathcal{P}_{e-})(1 + \mathcal{P}_{e+})\sigma_{LR} \}$$

- Unpolarized cross section:

$$\sigma_0 = \frac{1}{4} \{ \sigma_{RR} + \sigma_{LL} + \sigma_{RL} + \sigma_{LR} \}$$

- Left-right asymmetry:

$$A_{LR} = \frac{(\sigma_{LR} - \sigma_{RL})}{(\sigma_{LR} + \sigma_{RL})}$$

- Effective polarization and luminosity:

$$\mathcal{P}_{\text{eff}} = \frac{\mathcal{P}_{e-} - \mathcal{P}_{e+}}{1 - \mathcal{P}_{e-}\mathcal{P}_{e+}} \quad \mathcal{L}_{\text{eff}} = \frac{1}{2}(1 - \mathcal{P}_{e-}\mathcal{P}_{e+})\mathcal{L}$$

Statistical arguments

- Effective polarization

$$P_{eff} := (P_{e^-} - P_{e^+}) / (1 - P_{e^-} P_{e^+})$$








$$= (\#LR - \#RL) / (\#LR + \#RL)$$

'analyzing power'

- Fraction of colliding particles

$$\mathcal{L}_{eff} / \mathcal{L} := \frac{1}{2}(1 - P_{e^-} P_{e^+}) = (\#LR + \#RL) / (\#all)$$

'running time'

P_{e^-}	P_{e^+}		h_{e^-}	h_{e^+}	cross section	
-1	0		-1	+1	σ_{LR}	→ 0 ½ of events do not react !
			-1	-1	σ_{LL}	
+1	0		+1	-1	σ_{RL}	→ 0
			+1	+1	σ_{RR}	
-1	+1		-1	+1	σ_{LR}	
+1	-1		+1	+1	σ_{RL}	

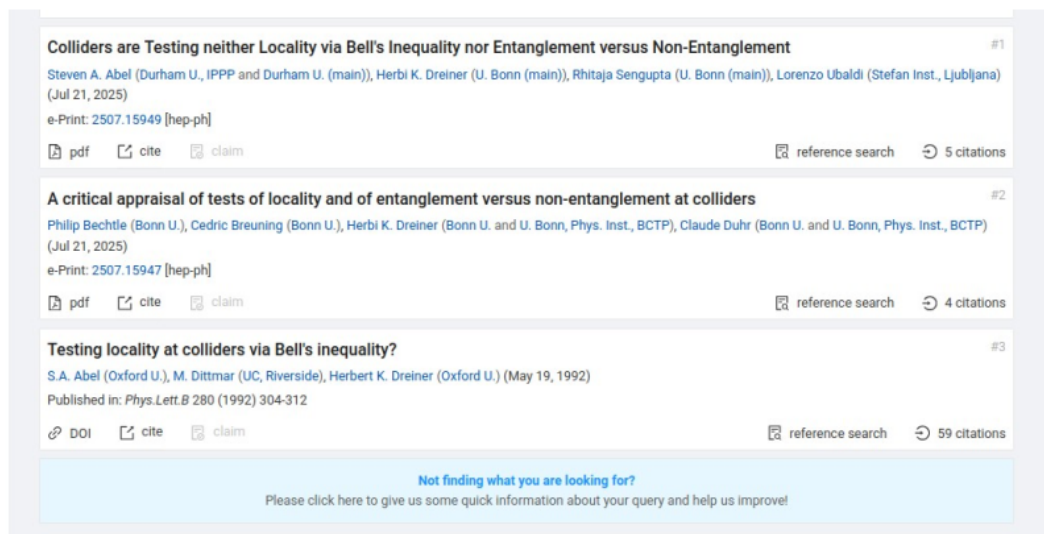
⇒ Enhancing of \mathcal{L}_{eff} with $P(e^-)$ and $P(e^+)$!

⇒ less running time only with both beams polarized !

A critical appraisal

Herbi Dreiner had tried all this at LEP in the 1990s

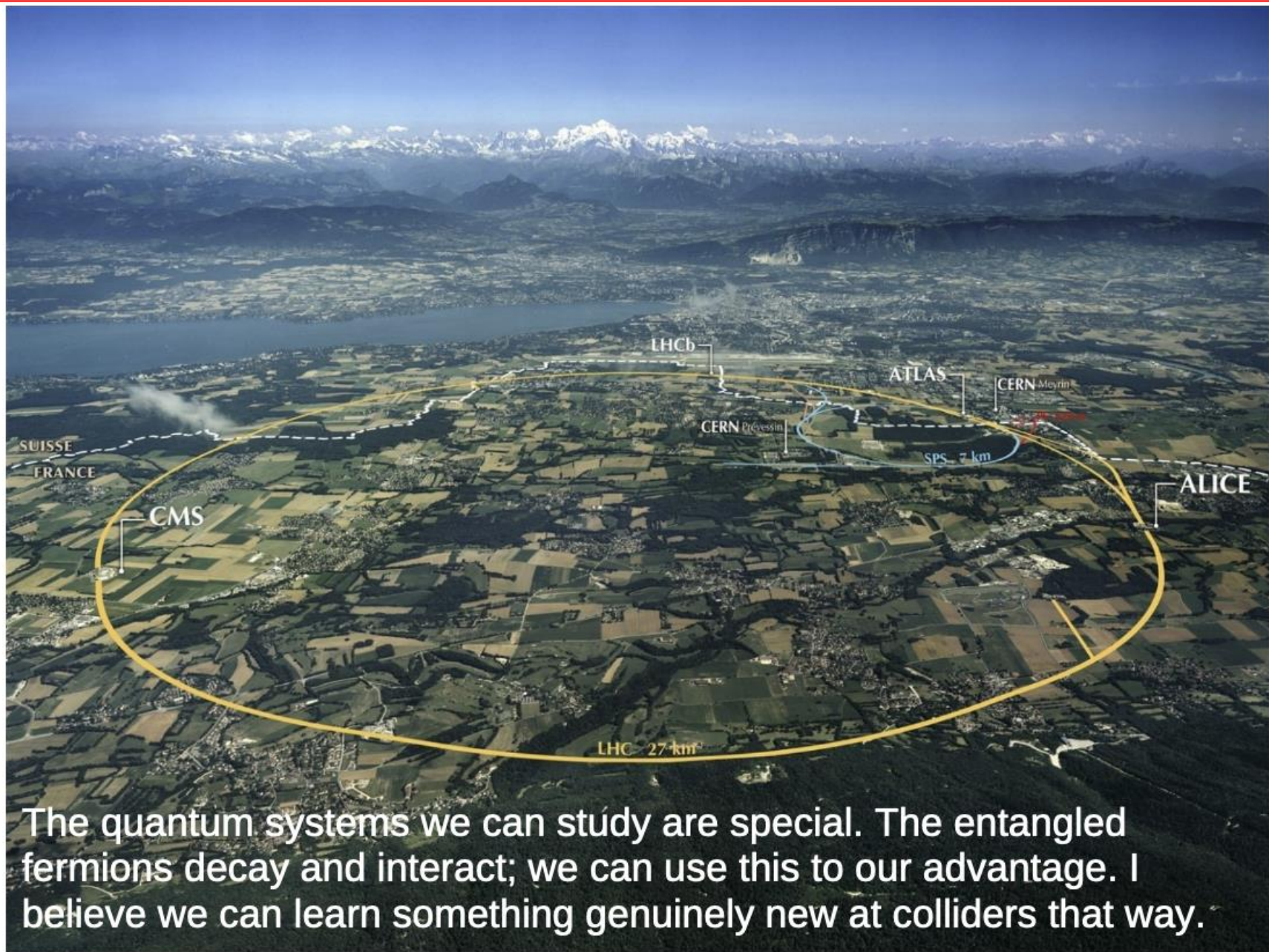
From M. Vos
@ Meeting of the Spanish network
for future colliders



The initial verdict: tests with commuting observables (momentum, not spin) can never rule out all hidden variable theories → locality cannot be tested conclusively

The more recent criticism: to probe the quantum (i.e. degree of entanglement) we rely on decays described by SM → nothing can be tested at colliders

Lesson: spell out assumptions more clearly, and test them in-situ (e.g. spin correlation in non-entangled region offers a control sample to test spin analyzing power)



From M. Vos @ Meeting of the Spanish network for future colliders

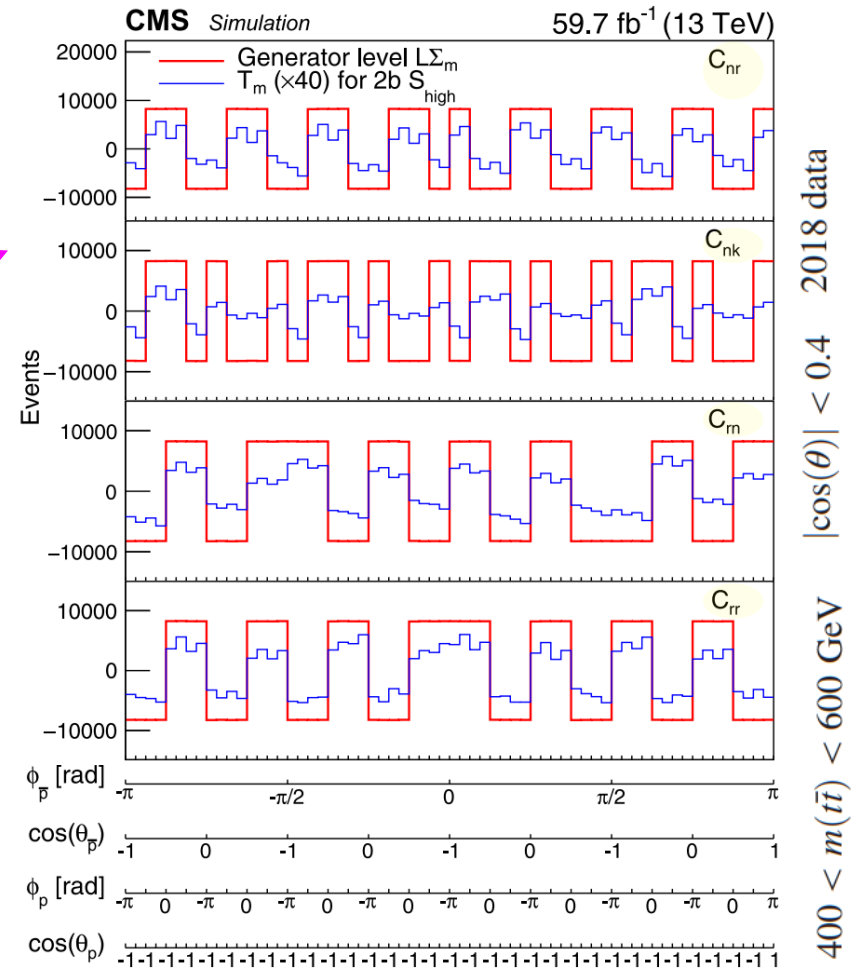
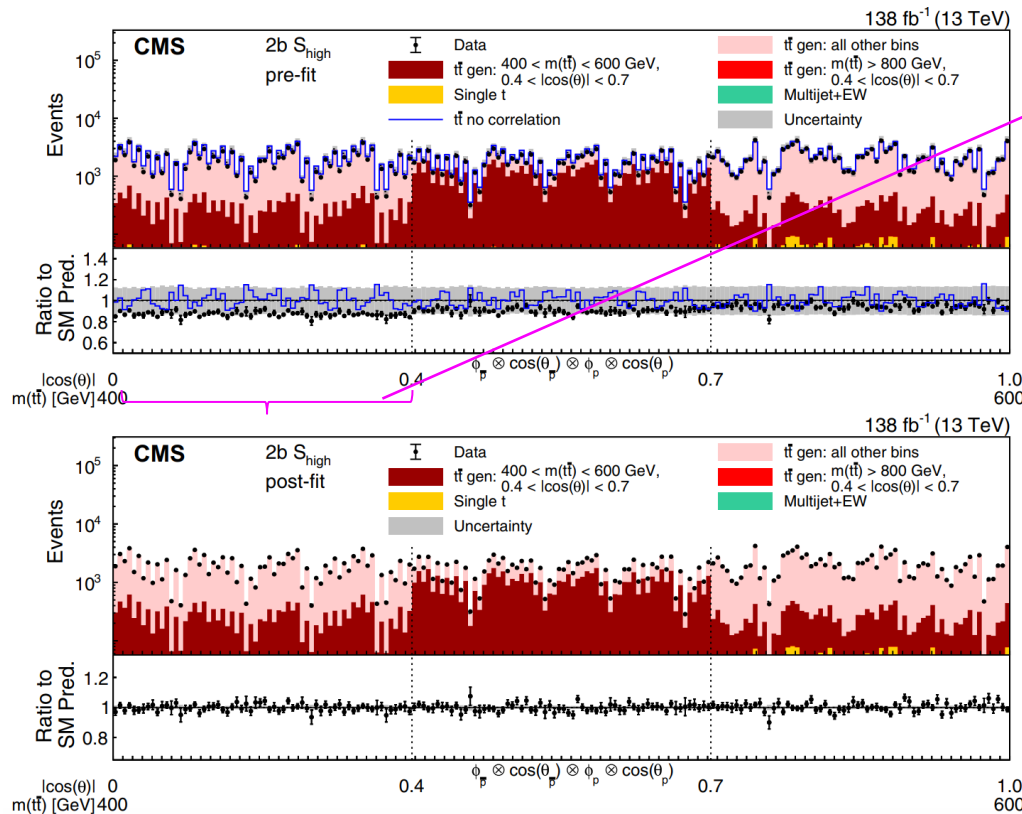
CMS lepton+jets channel: fits to various distributions

Binned maximum likelihood fit combining information of the 4 categories of various distributions in various regions of phase space - bins of $m_{t\bar{t}}/p_{T,t}$ and $\cos(\theta)$ -

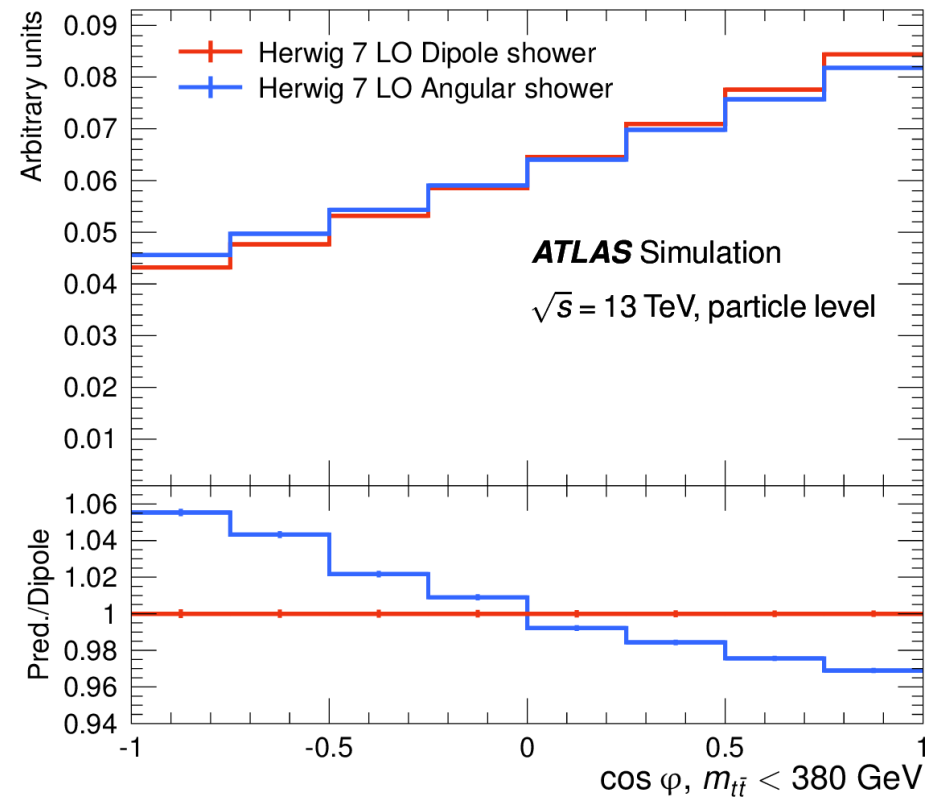
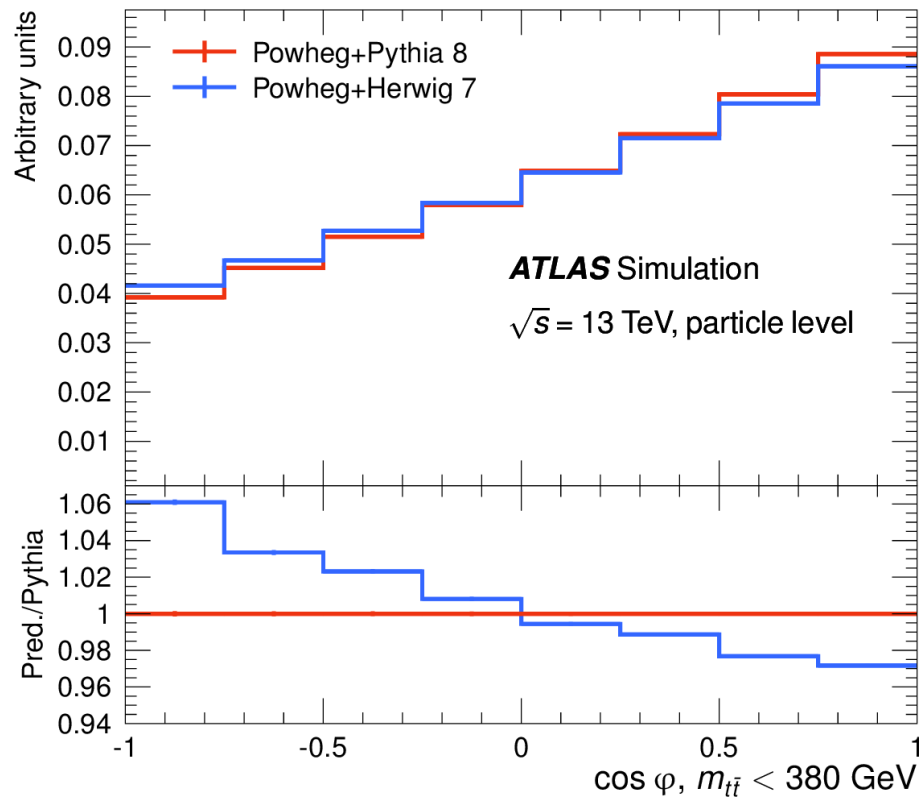
- unrolled 4D distribution of $\phi_{\bar{p}}, \cos(\theta_{\bar{p}}), \phi_p$, and $\cos(\theta_p) \rightarrow$ to extract full matrix coefficients
- $\cos(\chi)$ and $\cos(\tilde{\chi})$ distribution \rightarrow to study quantum entanglement

to reco-level templates (one for each coefficient)

from the outermost to the innermost variable $\phi_{\bar{p}}, \cos(\theta_{\bar{p}}), \phi_p$, and $\cos(\theta_p)$



ATLAS: 1st observation of entanglement in top quarks



Notable differences seen at particle-level for two different parton-shower models

Nature 633 (2024) 542

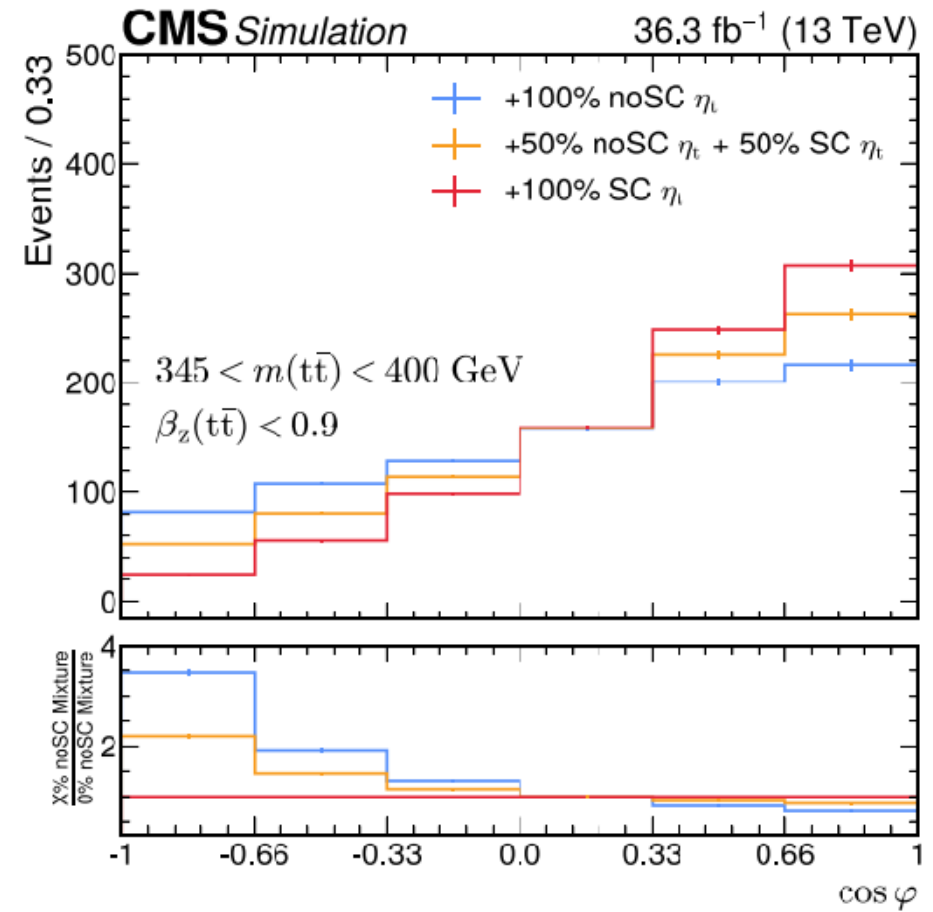
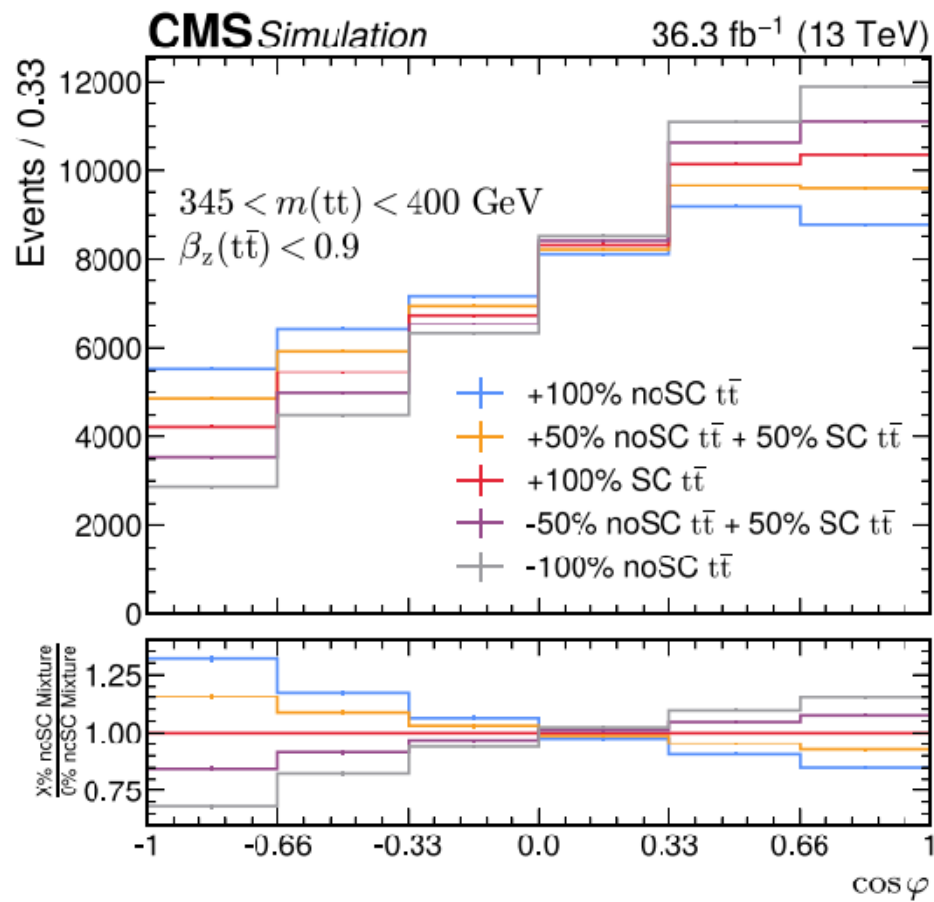
ATLAS: 1st observation of entanglement in top quarks

Nature 633 (2024) 542

Source of uncertainty	$\Delta D_{\text{observed}}(D = -0.537)$	ΔD [%]	$\Delta D_{\text{expected}}(D = -0.470)$	ΔD [%]
Signal modeling	0.017	3.2	0.015	3.2
Electrons	0.002	0.4	0.002	0.4
Muons	0.001	0.2	0.001	0.1
Jets	0.004	0.7	0.004	0.8
b -tagging	0.002	0.4	0.002	0.4
Pile-up	< 0.001	< 0.1	< 0.001	< 0.1
$E_{\text{T}}^{\text{miss}}$	0.002	0.4	0.002	0.4
Backgrounds	0.005	0.9	0.005	1.1
Total statistical uncertainty	0.002	0.3	0.002	0.4
Total systematic uncertainty	0.019	3.5	0.017	3.6
Total uncertainty	0.019	3.5	0.017	3.6

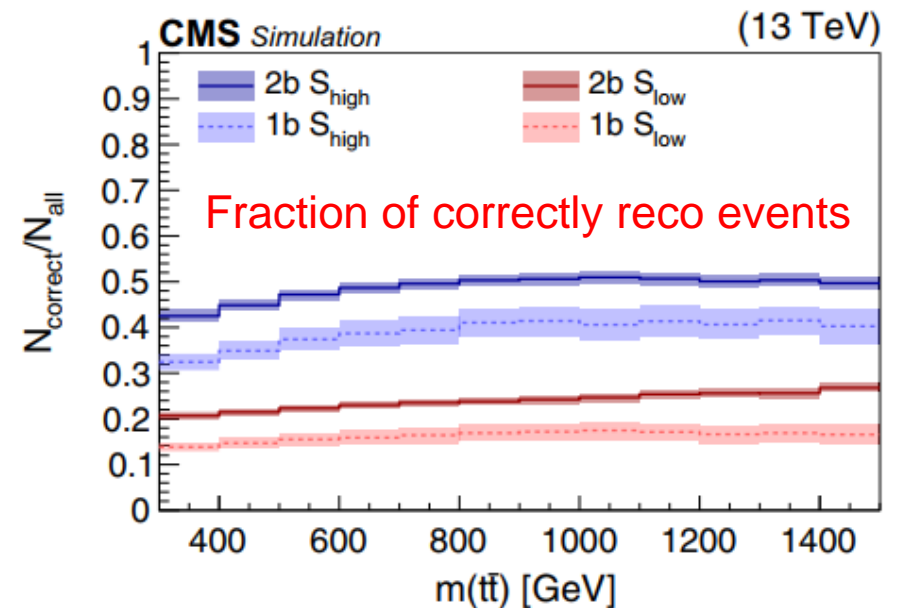
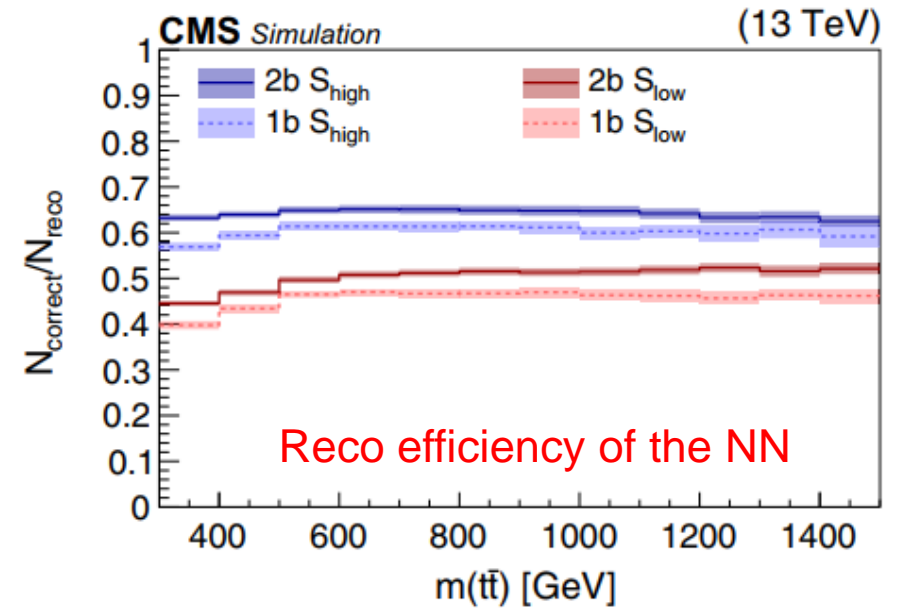
Systematic uncertainty source	Relative size (for SM D value)
Top-quark decay	1.6%
Parton distribution function	1.2%
Recoil scheme	1.1%
Final-state radiation	1.1%
Scale uncertainties	1.1%
NNLO QCD + NLO EW reweighting	1.1%
pT _{hard} setting	0.8%
Top-quark mass	0.7%
Initial-state radiation	0.2%
Parton shower and hadronization	0.2%
h_{damp} setting	0.1%

CMS threshold results using dilepton channel



The $2b$ and $1b$ categories are further split based on the value of S_{NN} . In the $1b$ ($2b$) category events belong to the S_{high} category if $S_{NN} > 0.30$ (0.36), while the remaining events are placed in the S_{low} category. These requirements define the signal categories for the analysis and were systematically optimized to minimize the uncertainties in the expected spin polarization and correlation coefficients.

In the simulation, the fraction of reconstructable $e/\mu +$ jets events is 73% for $2b S_{high}$, 47% for $2b S_{low}$, 64% for $1b S_{high}$, and 38% for $1b S_{low}$. The fractions of correctly reconstructed events with respect to all signal and background events in the various categories are 46% for $2b S_{high}$, 21% for $2b S_{low}$, 37% for $1b S_{high}$, and 15% for $1b S_{low}$. Figure 2 shows these fractions as functions of $m(t\bar{t})$ together with the fraction of correctly reconstructed events with respect to all reconstructable events.



Comparison with ATLAS

- Entanglement in top quark observed by both ATLAS and CMS with >5 standard deviations!
 - despite different analyses...

	ATLAS	CMS
Dataset	Full Run 2 (140 fb ⁻¹)	2016 (35.9 fb ⁻¹)
t \bar{t} decay	Dilepton: e μ	Dilepton: ee, e μ and $\mu\mu$
t \bar{t} reconstruction	Ellipse method	Weighting method
Main selections	340 < m(t \bar{t}) < 380 GeV	345 < m(t \bar{t}) < 400 GeV, beta < 0.9
Triggers	Single lepton	Single lepton + dilepton
Corrected to	Particle-level	Parton-level
Fit type	No fit, calibration curve	Profile likelihood template fit
Alternative hypothesis D	Reweighting	Mixing samples with/without spin corr
Threshold effects	Neglected	Considered (toponium contribution)
Nominal MC	PowhegBox+Pythia8	PowhegBox+Pythia8
Alternative MC	PowhegBox+Herwig7, bb4l	PowhegBox+Herwig++, MG5_AMC@NLO
Significance	>> 5 standard deviations	> 5 standard deviations

$$D_{obs} = -0.547 \pm 0.002(\text{stat}) \pm 0.021(\text{syst})$$

$$D_{exp} = -0.470 \pm 0.002(\text{stat}) \pm 0.018(\text{syst})$$

$$D_{obs} = -0.480^{+0.016}_{-0.017}(\text{stat})^{+0.020}_{-0.023}(\text{syst})$$

$$D_{exp} = -0.467^{+0.016}_{-0.017}(\text{stat})^{+0.021}_{-0.024}(\text{syst})$$

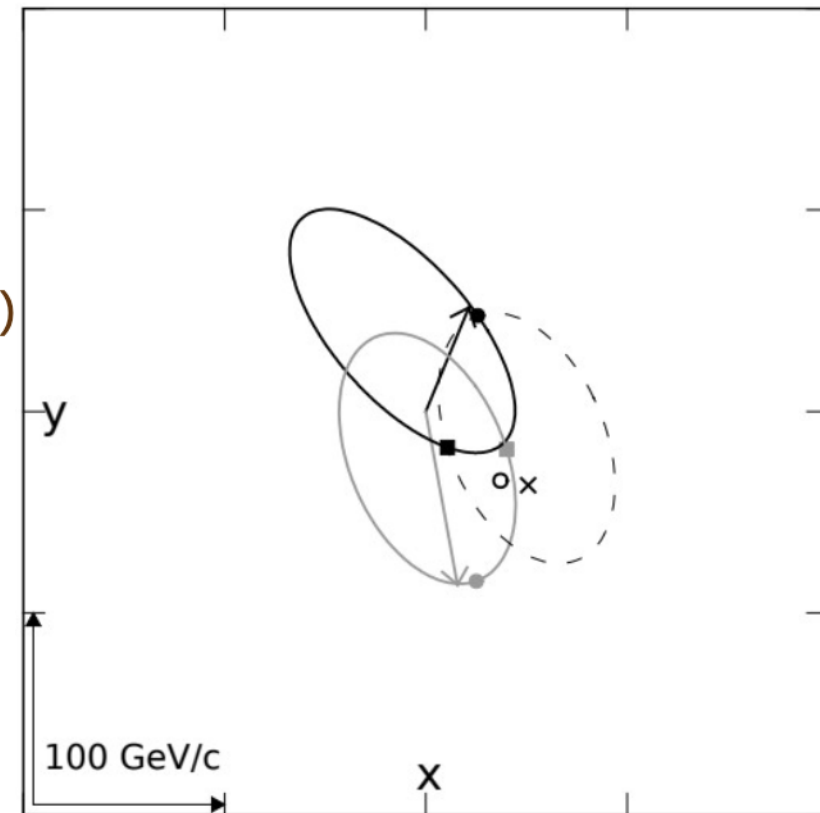
Top quark pair reconstruction

- Reconstruction of top quarks momenta complicated due to 2 neutrinos
 - Several methods were developed before, using $m(\text{top})$ and $m(W)$ as constraints

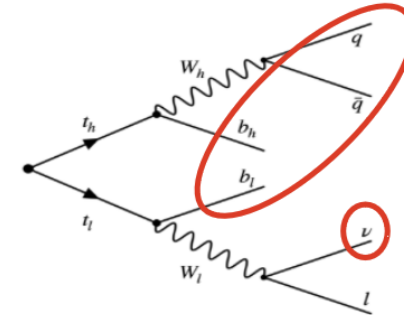
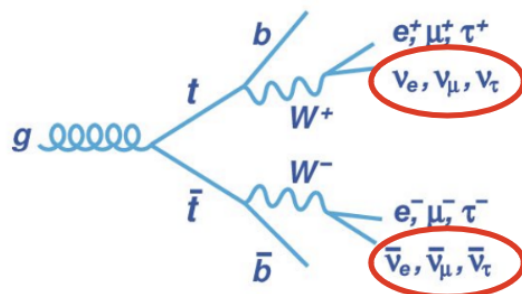
A combination of various methods used:

- Main method: **'Ellipse' method** (85% effic.)
 - Analytically calculate two ellipses for $p_T(\nu)$ and find intersections
- If 'Ellipse' fails → **'Neutrino Weighting' method** (5%)
 - Scans $\eta(\nu)$, $\eta(\bar{\nu})$ phase-space
 - Solutions weighted based on compatibility between p_T of neutrinos and missing p_T
- If both methods fail: **simple pairing** of leptons with the closest b-jets (10%)
 - Use highest- p_T jet if only 1 b-tagged jet

NIM A 736 (2014) 169-178



Dilepton vs lepton+jets top quark reconstruction



• $m_{\ell b}$ weighting method

- use algebraic method to solve for neutrino 3-vectors
- pick solution with smallest $m_{t\bar{t}}$
- pair lepton and jet according to expected $m_{\ell b}$

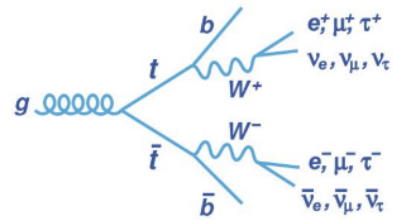
$$\begin{aligned} E_x &= p_{\nu_x} + p_{\bar{\nu}_x} \\ E_y &= p_{\nu_y} + p_{\bar{\nu}_y} \end{aligned}$$

$$\begin{aligned} m_{W^+}^2 &= (E_{\ell^+} + E_{\nu})^2 - (p_{\ell^+_x} + p_{\nu_x})^2, \\ &\quad - (p_{\ell^+_y} + p_{\nu_y})^2 - (p_{\ell^+_z} + p_{\nu_z})^2, \\ m_{W^-}^2 &= (E_{\ell^-} + E_{\bar{\nu}})^2 - (p_{\ell^-_x} + p_{\bar{\nu}_x})^2, \\ &\quad - (p_{\ell^-_y} + p_{\bar{\nu}_y})^2 - (p_{\ell^-_z} + p_{\bar{\nu}_z})^2, \\ m_t^2 &= (E_b + E_{\ell^+} + E_{\nu})^2 - (p_{b_x} + p_{\ell^+_x} + p_{\nu_x})^2, \\ &\quad - (p_{b_y} + p_{\ell^+_y} + p_{\nu_y})^2 - (p_{b_z} + p_{\ell^+_z} + p_{\nu_z})^2, \\ m_{\bar{t}}^2 &= (E_{\bar{b}} + E_{\ell^-} + E_{\bar{\nu}})^2 - (p_{\bar{b}_x} + p_{\ell^-_x} + p_{\bar{\nu}_x})^2, \\ &\quad - (p_{\bar{b}_y} + p_{\ell^-_y} + p_{\bar{\nu}_y})^2 - (p_{\bar{b}_z} + p_{\ell^-_z} + p_{\bar{\nu}_z})^2. \end{aligned}$$

• Artificial NN

- goal = correctly identify detector-level objects and up/down jet assignment
- NN trained on permutations
- For each event:
 - provide all possible permutations of objects as input to NN
 - use permutation resulting in the highest NN score
 - calculate neutrino momentum with W boson mass constraint

$$(p_\nu + p_l)^2 = m_W^2$$



Dilepton vs lepton+jets

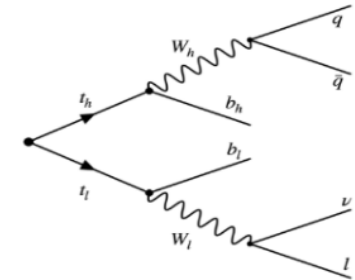
Dilepton

[arXiv:2406.03976](https://arxiv.org/abs/2406.03976)
accepted by ROPP

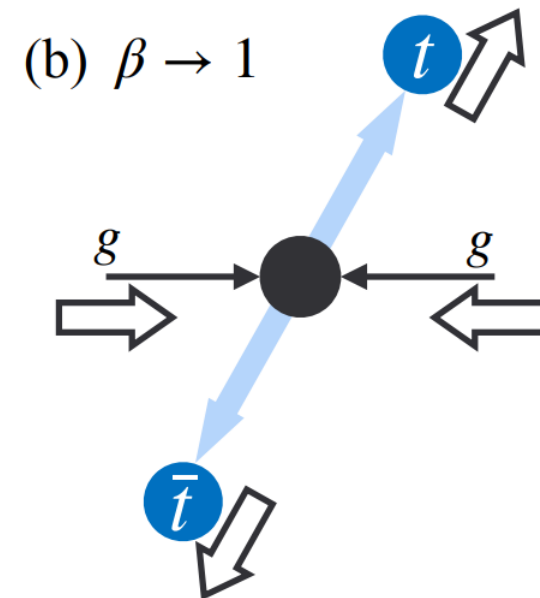
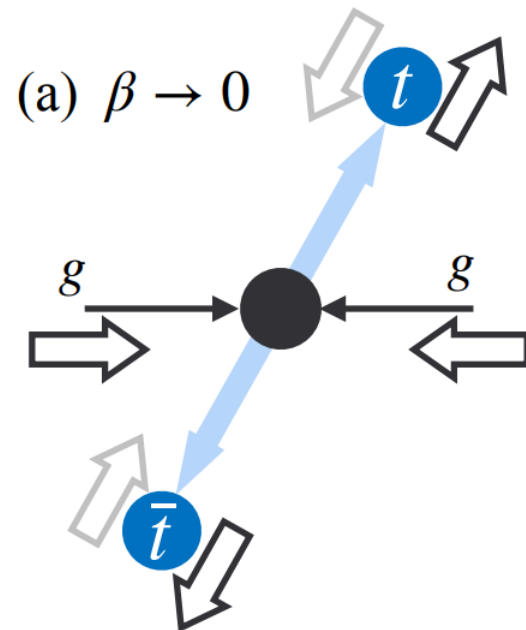
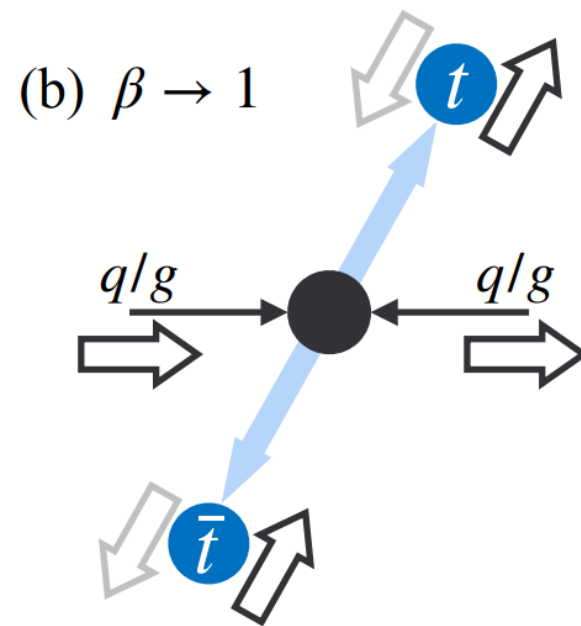
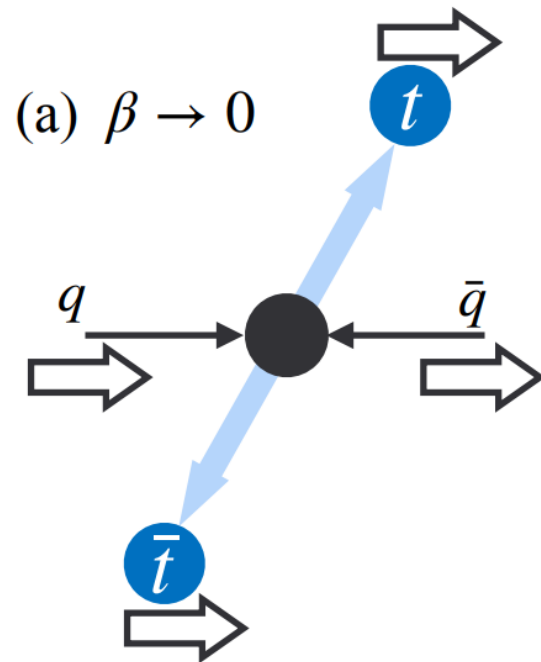
- **36.3 fb⁻¹ of 2016 data @13 TeV**
 - based on [PRD 100 \(2019\) 072002](https://arxiv.org/abs/1907.07200)
- Lower branching ratio
- top spin info 100 % transmitted to charged leptons → **easy to identify**
- Lower p_T cuts for leading/subleading lepton (25/20 GeV) → **higher efficiency** at the threshold
- Worse $m_{t\bar{t}}$ resolution → not ideal for differential measurement
- **Best for threshold region**
 - high entanglement
 - mostly **time-like separated events**

Lepton + jets

[arXiv:2409.11067](https://arxiv.org/abs/2409.11067)
submitted to PRD



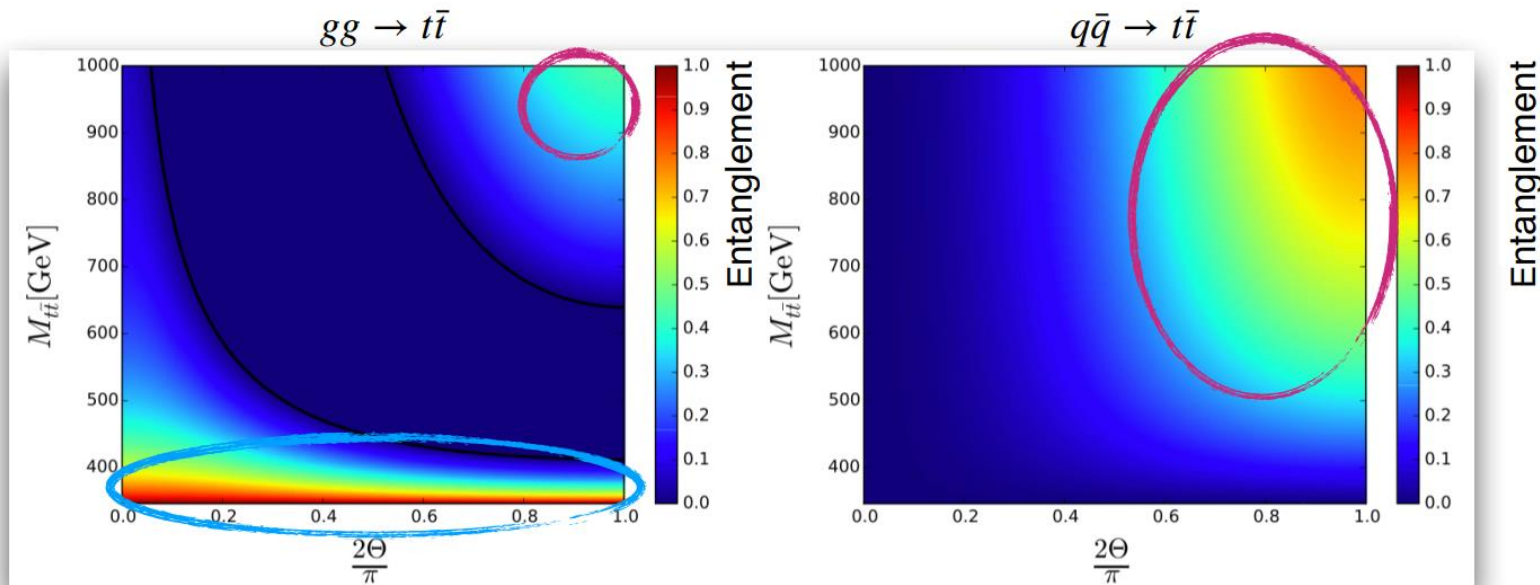
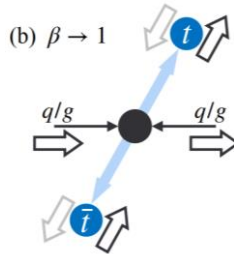
- **138 fb⁻¹ of data @13 TeV** collected in full Run 2
- **Higher branching ratio**
- top spin info ~100 % transmitted to down-type quarks → hard to identify
- Higher p_T cut for single lepton (30 GeV) and for 4 jets (30 GeV) → lower efficiency at the threshold but OK for high $m_{t\bar{t}}$
- **Better $m_{t\bar{t}}$ resolution** → good for differential measurement
- **Advantage for high $m_{t\bar{t}}$**
 - high entanglement
 - mostly **space-like separated events**



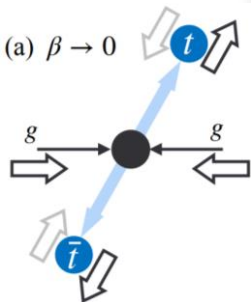
Entanglement of top quarks

- Can be measured using **spin correlations variables**
- Depends on production mode, $m_{t\bar{t}}$, scattering angle of the top quark (Θ)
- SM predicts entangled states:
 - at the **production threshold region** in gg fusion production
 - at the **boosted region for central production** of the $t\bar{t}$ system

high relative velocity
of top quarks
→ **space-like
separated** events



low relative velocity of top quarks
→ **time-like separated** events



Afik, De Nova
[Eur. Phys. J. Plus **136**, 907](#)

How to probe entanglement

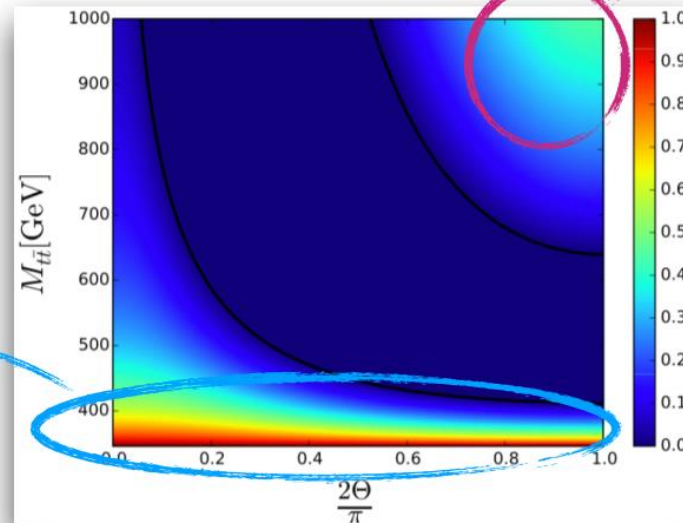
- Four maximally entangled states:

$$|\Phi^\pm\rangle = \frac{1}{\sqrt{2}}(|\uparrow\uparrow\rangle \pm |\downarrow\downarrow\rangle)$$

$$|\Psi^\pm\rangle = \frac{1}{\sqrt{2}}(|\uparrow\downarrow\rangle \pm |\downarrow\uparrow\rangle)$$

$gg \rightarrow t\bar{t}$

Afik, De Nova
Eur. Phys. J. Plus **136**, 907



- Spin-singlet pseudoscalar state Ψ^-

- At low $m_{t\bar{t}}$: $C_{rr} > 0$ and $C_{kk} > 0$

$$\Delta_E = C_{nn} + C_{rr} + C_{kk} = \text{Tr}[C] = -3D > 1$$

$$D = -\frac{\text{tr}[C]}{3} \rightarrow D < -1/3$$

- Spin-triplet vector state ($\Phi^+ - \Phi^-$, Ψ^+ , $\Phi^+ + \Phi^-$)
- At high $m_{t\bar{t}}$ and low $|\cos \Theta|$: $C_{kk} < 0$ and $C_{rr} < 0$

$$\Delta_E = C_{nn} - C_{rr} - C_{kk} = 3\tilde{D} > 1$$

$$\rightarrow \tilde{D} > 1/3$$

$$\Delta_E = C_{nn} + |C_{rr} + C_{kk}| > 1$$

Sufficient condition for entanglement

→ measure D, \tilde{D} to access entanglement information in top quark events!